Erstgutachterin: PD Dr. Jeanette Lorenz
Zweitgutachter: Prof. Dr. Wolfgang Dünnweber

Search for charginos and neutralinos in a signature with a Higgs boson and an isolated lepton with the ATLAS detector and its reinterpretation in the phenomenological MSSM

Thesis submitted for a doctoral degree in physics
at the faculty of physics of the
Ludwig-Maximilians University
Munich, Germany

Submitted by Eric Schanet, born in Luxembourg,
on May 4th, 2021

Supported by the Luxembourg National Research Fund (FNR) (13562317)

Part I

Fundamental concepts

Part II

The 1-lepton analysis

Part III

Reinterpretation

Chapter 11

Reinterpretation in the pMSSM

After having discussed methods and approaches to reinterpret ATLAS searches for Supersymmetry (SUSY), this chapter exploits the analysis approximations previously introduced, and presents a re-interpretation of the 1ℓ search in the phenomenological Minimal Supersymmetric Standard Model (pMSSM).

11.1 Motivation

In today's searches for SUSY, it is common to use simplified models as a way of avoiding the necessity of having to deal with high-dimensional parameter spaces that are extremely challenging to sample and compare to data. As has been discussed in sections 1.2.7 and 8.3, simplified models are however by no means complete SUSY models, but only serve as proxies for more complex and realistic SUSY scenarios. As such, simplified model limits cannot trivially be translated into limits on model parameters of a more complete SUSY model, and large-scale reinterpretations are necessary to understand the constraints current SUSY searches set on realistic SUSY scenarios.

One class of more complete models, focussing on phenomenologically viable models, is the pMSSM, introduced in section 1.2.6. With its 19 parameters it offers much more complex SUSY scenarios, while still being of somewhat manageable dimensionality. Still, large-scale reinterpretations in the pMSSM are computationally challenging and require a set of approximations as those introduced in chapters 9 and 10. In the following, the *simplified analysis* constructed using the smeared truth-level analysis and the simplified likelihood will be used as the sole method to evaluate a set of pMSSM models.

Although the following sections will be restricted to a reinterpretation of the 1ℓ search, efforts are ongoing within the ATLAS collaboration to perform large-scale reinterpretations using a majority of the Run 2 ATLAS searches for SUSY, most likely resulting in one of the most comprehensive sets of ATLAS constraints on SUSY yet.

Table 11.1: Scan ranges used for each of the 19 pMSSM parameters. For parameters written with a modulus sign, both the positive and negative values are allowed. The term 'gen(s)' refers to generation(s). Flat probability distributions are used to sample random values from the given ranges.

Parameter	min	max	Note
$m_{\tilde{L}_1}$ $(= m_{\tilde{L}_2})$	10 TeV	10 TeV	Left-handed slepton (first two gens.) mass
$m_{\tilde{e}_1}$ $(= m_{\tilde{e}_2})$	10 TeV	10 TeV	Right-handed slepton (first two gens.) mass
$m_{\tilde{L}_3}$	10 TeV	10 TeV	Left-handed stau doublet mass
$m_{\tilde{e}_3}$	10 TeV	10 TeV	Right-handed stau mass
$m_{\tilde{Q}_1}$ $(= m_{\tilde{Q}_2})$	10 TeV	10 TeV	Left-handed squark (first two gens.) mass
$m_{\tilde{u}_1}$ $(= m_{\tilde{u}_2})$	10 TeV	10 TeV	Right-handed up-type squark (first two gens.) mass
$m_{\tilde{d}_1}$ $(= m_{\tilde{d}_2})$	10 TeV	10 TeV	Right-handed down-type squark (first two gens.) mass
$m_{\tilde{Q}_3}$	2 TeV	5 TeV	Left-handed squark (third gen.) mass
$m_{\tilde{u}_3}$	2 TeV	5 TeV	Right-handed top squark mass
$m_{\tilde{d}_3}$	2 TeV	5 TeV	Right-handed bottom squark mass
$\lvert M_1 \rvert$	0 TeV	2 TeV	Bino mass parameter
$\lvert M_2 \rvert$	0 TeV	2 TeV	Wino mass parameter
$\lvert \mu \rvert$	0 TeV	2 TeV	Bilinear Higgs mass parameter
M_3	1 TeV	5 TeV	Gluino mass parameter
$\lvert A_t \rvert$	0 TeV	8 TeV	Trilinear top coupling
$\lvert A_b \rvert$	0 TeV	2 TeV	Trilinear bottom coupling
$\lvert A_\tau \rvert$	0 TeV	2 TeV	Trilinear τ lepton coupling
M_A	0 TeV	5 TeV	Pseudoscalar Higgs boson mass
$\tan\beta$	1	60	Ratio of the Higgs vacuum expectation values

11.2 Model sampling and processing

11.2.1 Sampling

All signal models considered in the following are sampled from the pMSSM using the parameter ranges shown in table 11.1. Flat probability distributions are used to draw random values within the given ranges for each parameter and each unique set of pMSSM parameters generated that way is referred to as an independent pMSSM model.

As this work discusses a search for electroweakinos, the models drawn from the pMSSM are sampled with a special focus on the electroweak sector. This is achieved by setting the mass parameters of the first and second generation squarks to values much higher than those accessible at Large Hadron Collider (LHC) energies, effectively decoupling them. Likewise, sleptons are also effectively decoupled because the 1ℓ search is not expected to be sensitive to slepton pair production or scenarios with sleptons in the decay chains. For naturalness arguments, third generation squarks and the gluino are not strictly decoupled, but set to sufficiently high values such as not to affect the electroweak sector too much. The lower and upper bounds on the 12 scanned parameters are chosen such as to yield a high density of models with electroweakino masses accessible at LHC energies, while allowing the scan to be as general as possible.

Once a value for each of the 19 pMSSM parameters has been chosen, a number of publicly available software packages are executed in order to compute the properties of each model. In a first step, SPheno v4.0.5 [290, 291] is used to calculate the spectrum of the sparticles, which, in turn, serves as input for determining the masses and branching fractions of the Higgs sector using FeynHiggs v2.15.0 [292–294]. An additional SUSY spectrum calculation is performed in parallel with SoftSusy v4.1.8 [295]. Although the spectra obtained from SoftSusy will not be directly used in the following, the program is still required to complete successfully in order to reduce the number of pMSSM models with pathological properties. After the complete model spectrum has been calculated, the dark matter relic abundance of each model is determined with micrOMEGAs v5.0.8 [296, 297].

11.2.2 Selection and processing

In order to avoid models with pathological properties, all spectrum generators and additional programs are required to complete execution without error. The cross sections for surviving models are computed at next-to-leading order (NLO) using Prospino v2.1 [298, 299]. Models with inclusive cross sections for all electroweakino production processes below 0.07 fb are discarded as they would result in less than 10 expected signal events with an integrated luminosity of $139\,\text{fb}^{-1}$, which is not sufficient to be sensitive to with current electroweak SUSY searches. All models are further required to produce a lightest Higgs boson mass compatible within a ± 5 GeV range with the experimentally measured Standard Model (SM) Higgs boson mass[†]. Models where the $\tilde{\chi}_1^0$ is not the lightest supersymmetric particle (LSP) are also rejected.

No constraints on the computed cosmological LSP abundance are applied at this stage in order to give a more general view after the models are evaluated using the 1ℓ search. For the same reason,

[†] The mass range is based on a conservative estimate of the theoretical uncertainties arising from the FeynHiggs calculation.

experimental constraints like the lower limit on the chargino mass from Large Electron Positron (LEP) are also not applied at this stage.

Of the 10,000 unique models sampled from the pMSSM using the above prescription, 5152 models survive the constraints and requirements discussed in this section and are analysed using the simplified 1ℓ search. The majority of the models failing this selection step were rejected due to the cross section constraint.

11.2.3 Event generation

Event generation is performed using the software centrally provided by the ATLAS production system. The initial pair of sparticles with up to one additional parton in the matrix element are generated using the MadGraph5_aMC@NLO v2.6.1. [187, 188] generator. Next, Pythia8.230 [190] with the A14 [191] tune is used for the hadronisation and parton showering, together with the NNPDF 2.3 LO [189] parton distribution function (PDF) set. The number of events N generated for each model is determined by

$$N = \sigma \times \mathcal{L}_{\text{eff}}, \tag{11.1}$$

where $\mathcal{L}_{\text{eff}} = 700\,\text{fb}^{-1}$ is an effective integrated luminosity and σ is the total production cross section of the model. The number of events generated for each model is capped at a minimum number of 10^4 and a maximum number of 10^6 truth-level events.

11.2.4 Truth-level analysis

All models passing event generation are evaluated using the simplified analysis comprised of truth-level inputs, four-vector smearing and the simplified likelihood. This is the only evaluation done for the models considered herein. A full scan over the pMSSM including multiple ATLAS searches would additionally include a processing step reverting back to the full analysis available through Recast for model points where (non-)exclusion is uncertain based on the simplified analysis only.

11.3 Phenomenology of the LSP

The composition of the $\tilde{\chi}_1^0$ in each pMSSM model sampled is shown in projections onto the $m(\tilde{\chi}_1^\pm)$–$m(\tilde{\chi}_1^0)$ and $m(\tilde{\chi}_2^0)$–$m(\tilde{\chi}_1^0)$ planes in figs. 11.1(a) and 11.1(b), respectively. The $\tilde{\chi}_1^0$ is considered to be bino-like ($\tilde{B}$-like), wino-like ($\tilde{W}$-like) or higgsino-like ($\tilde{H}$-like) if the corresponding fraction from the neutralino mass mixing matrix is at least 80%. If more than one component has a fraction of more than 20%, then the $\tilde{\chi}_1^0$ is considered to be of mixed nature. For example, a $\tilde{\chi}_1^0$ with more than 20% bino-, wino- and higgsino-components is referred to as $\tilde{B}\tilde{W}\tilde{H}$-like. The nature of the LSP as a function of the bino, wino and higgsino mass parameters (M_1, M_2 and μ) is shown as a reference in fig. C.2.

In the bulk of the $m(\tilde{\chi}_1^\pm)$–$m(\tilde{\chi}_1^0)$ plane, i.e. the parameter space targeted by the 1ℓ search using the simplified model, a large majority of the models produce a bino-like LSP with nearly mass-degenerate $\tilde{\chi}_1^\pm$ and $\tilde{\chi}_2^0$. These models correspond to cases where $M_1 \ll \mu$ and $M_1 < M_2$ and thus produce electroweakino spectra similar to the canonical simplified model considered in the 1ℓ search. Some sensitivity can therefore be expected towards these models in the context of the 1ℓ search, provided

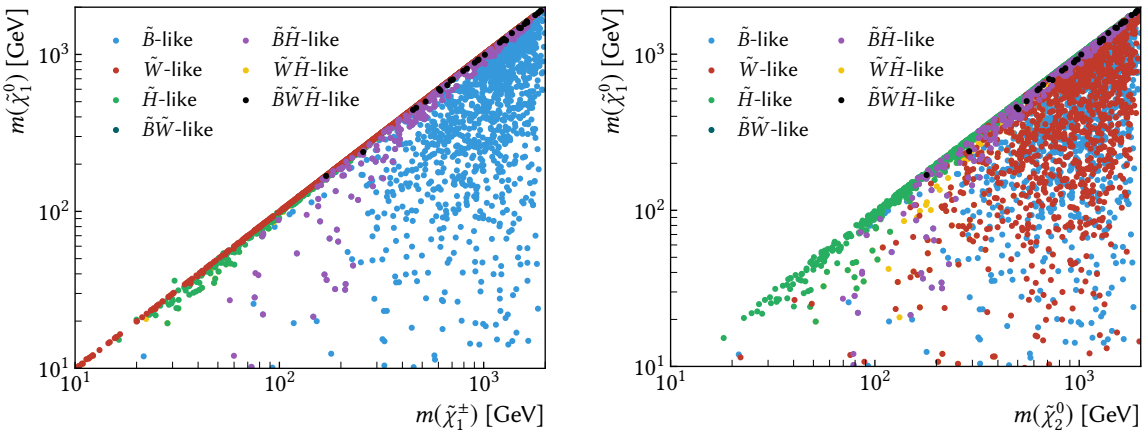

(a) $m(\tilde{\chi}_1^\pm)$–$m(\tilde{\chi}_1^0)$ plane **(b)** $m(\tilde{\chi}_2^0)$–$m(\tilde{\chi}_1^0)$ plane

Figure 11.1: Projections of all models sampled onto the (a) $m(\tilde{\chi}_1^\pm)$–$m(\tilde{\chi}_1^0)$ and (b) $m(\tilde{\chi}_2^0)$–$m(\tilde{\chi}_1^0)$ planes. Each point represents a distinct pMSSM model with a unique combination of pMSSM parameters. The colour encodes the composition of the $\tilde{\chi}_1^0$ in each model. Details on how the LSP type is defined are given in the text.

that the decays $\tilde{\chi}_1^\pm \to W^\pm \tilde{\chi}_1^0$ and $\tilde{\chi}_2^0 \to h\tilde{\chi}_1^0$ have sufficiently large branching fractions and produce on-shell bosons.

Towards the diagonal of the $m(\tilde{\chi}_1^\pm)$–$m(\tilde{\chi}_1^0)$ plane, i.e. for models with nearly mass-degenerate $\tilde{\chi}_1^\pm$ and $\tilde{\chi}_1^0$, the nature of the LSP shows a larger variation. In a large set of models where M_2 is not too large and much smaller than M_1 and μ, the LSP has a significant wino component and is nearly mass-degenerate with the $\tilde{\chi}_1^\pm$, while the $\tilde{\chi}_2^0$ and other electroweakinos can be more massive. In models where the LSP has a large higgsino component, i.e. μ is much smaller than M_1 and M_2, the three electroweakinos $\tilde{\chi}_1^\pm$, $\tilde{\chi}_2^0$ and $\tilde{\chi}_1^0$ are nearly mass-degenerate and, if promptly decaying, result in very soft decay products, making these models inherently difficult to target.

11.4 Impact of the 1ℓ search on the pMSSM

In the following sections, the impact of the 1ℓ search on the pMSSM is discussed using one-dimensional and two-dimensional projections and distributions. A model is considered to be excluded if the observed CL_s value obtained with the simplified likelihood using the smeared truth-level inputs and the simplified likelihood is below 0.05. Of the 5152 models evaluated, the 1ℓ search excludes a total of 98, or about 1.9%, of the models.

For the one-dimensional distributions shown in the following, the total number of models is compared against the number of models excluded by the 1ℓ search. An additional pad indicates the ratio between models excluded and total models sampled in each bin of the distribution. In the two-dimensional projections, the numbers in the bins indicate the number of pMSSM models sampled in each bin. In these projections, the bin-wise fraction of models excluded with the 1ℓ search is colour-encoded. Bins in which all models are excluded are coloured in black, while bins without any excluded models are left white. Where applicable, the exclusion contour obtained by the 1ℓ search in the simplified model scenario is overlaid.

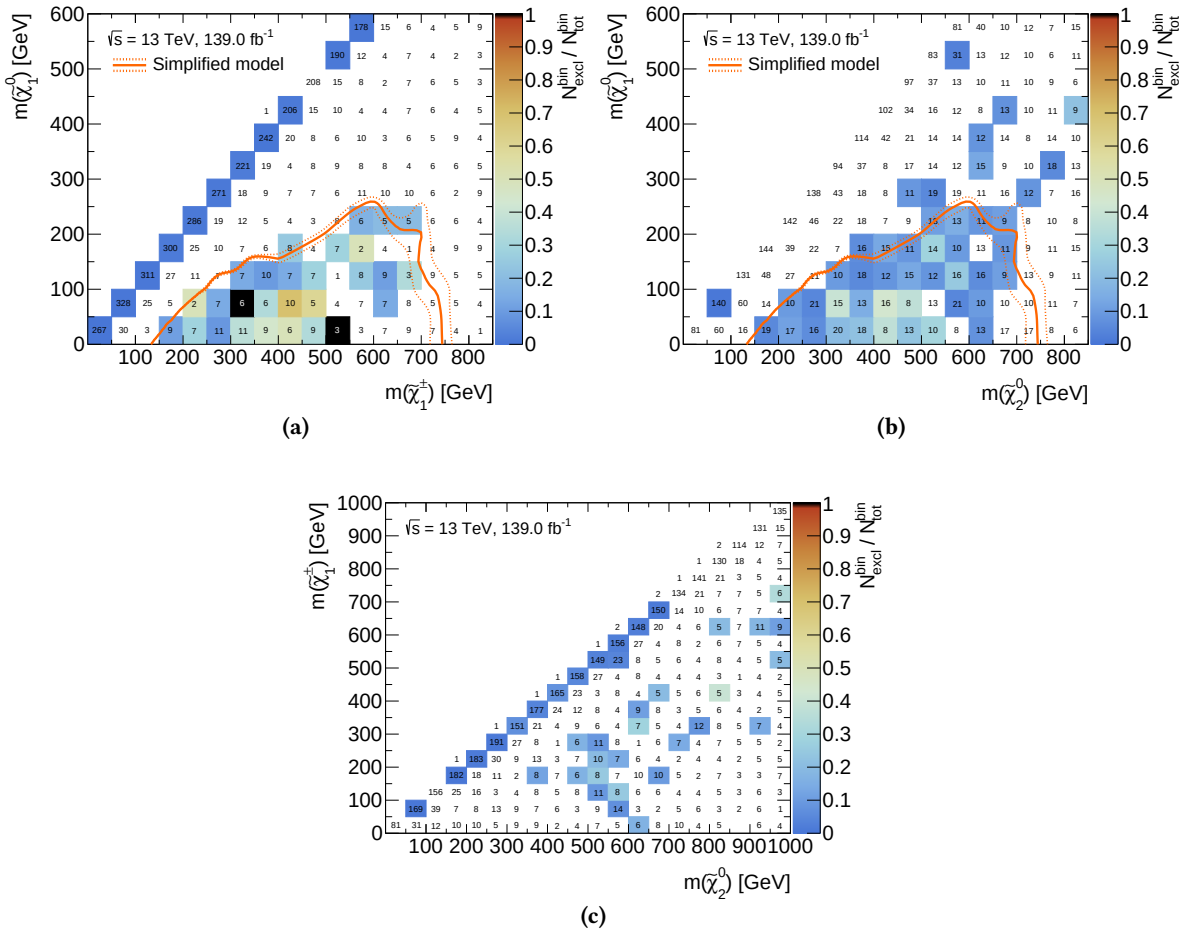

Figure 11.2: Bin-by-bin fraction of excluded models as a function of the relevant sparticle masses. The numbers in the bins correspond to the total number of models sampled in the respective bin. The bin-wise fraction of models excluded by the 1ℓ search is encoded with a colour bar ranging from 0 to 1. Where all models in a given bin are excluded, the bin is coloured in black. Bins without any models excluded are left white. Models are evaluated using the simplified likelihood of the 1ℓ search. Where applicable, the simplified model contour is shown in orange.

11.4.1 Impact on electroweakino masses

Figures 11.2 and 11.3 show the bin-by-bin fractions of models excluded by the 1ℓ search as two- and one-dimensional distributions, respectively. From the $\tilde{\chi}_1^{\pm}$–$\tilde{\chi}_1^0$ plane in fig. 11.2(a), it can be observed that the 1ℓ search is most sensitive to pMSSM models in electroweakino mass ranges similar to those excluded in the context of the simplified model. Most of the models excluded have $\tilde{\chi}_1^{\pm}/\tilde{\chi}_2^0$ masses ranging from roughly 200 GeV to about 700 GeV, and $\tilde{\chi}_1^0$ masses ranging masses from 0 GeV to about 300 GeV. The proportion of excluded models peaks at $m(\tilde{\chi}_1^{\pm}/\tilde{\chi}_2^0) \approx 450$ GeV and light LSPs with $\tilde{\chi}_1^0 < 150$ GeV, as visible in fig. 11.3.

The models excluded by the 1ℓ search can be classified in two broad categories: models situated within the parameter range enclosed by the simplified model exclusion contour, and models with nearly mass-degenerate $\tilde{\chi}_1^{\pm}$ and $\tilde{\chi}_2^0$. As discussed in section 11.3, most models within the simplified model

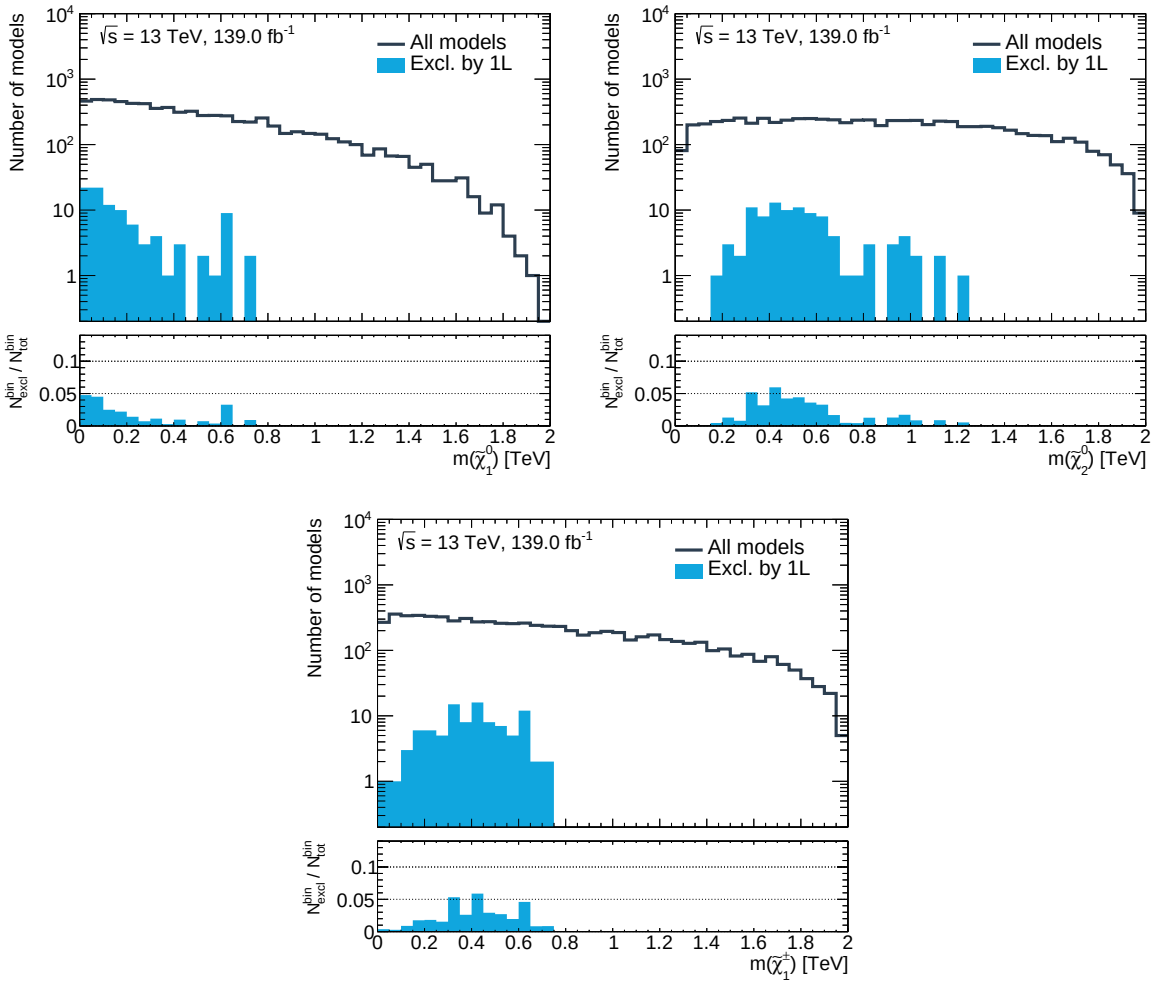

Figure 11.3: Bin-by-bin number of excluded models as a one-dimensional function of the electroweakino masses. The bin-wise fraction of excluded models, $N^{\text{bin}}_{\text{excl}}/N^{\text{bin}}_{\text{total}}$, is shown in the lower pad. All models are evaluated using the simplified likelihood of the 1ℓ search.

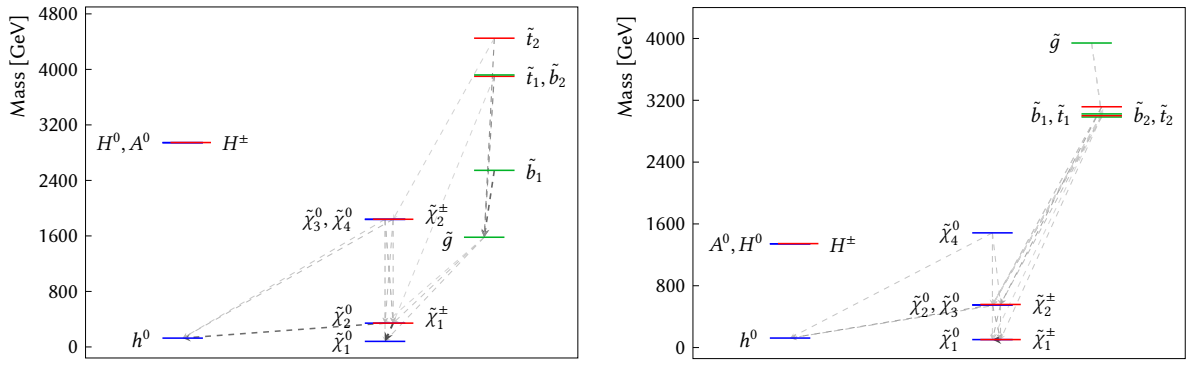

(a) Bino-like $\tilde{\chi}_1^0$ model

(b) Wino-like $\tilde{\chi}_1^0$ model

Figure 11.4: Mass spectra of two exemplary pMSSM models. Both models are excluded by the 1ℓ search. Fig. (a) represents a model with a bino-like LSP and nearly mass-degenerate $\tilde{\chi}_1^\pm$ and $\tilde{\chi}_2^0$. In fig. (b), a model with a wino-like LSP and mass-degenerate $\tilde{\chi}_1^\pm$ and $\tilde{\chi}_2^0$ but relatively light $\tilde{\chi}_2^\pm$ (nearly mass-degenerate with the $\tilde{\chi}_2^0$) is shown. The branching fractions of the different decays are indicated through the width and greyscale colour (pure black being 100% BF, pure white being 0% BF) of the arrows. Branching fractions below 10% are suppressed for the sake of visibility. Figures generated using `pyslha` [92].

exclusion contour produce a bino-like LSP and result in nearly mass-degenerate[†] $\tilde{\chi}_1^\pm$ and $\tilde{\chi}_2^0$. Expectedly, the 1ℓ search shows sensitivity to $\tilde{\chi}_1^\pm\tilde{\chi}_2^0$ production in models with wino-like electroweakinos and a bino-like $\tilde{\chi}_1^0$, resulting in spectra close to that of the canonical simplified model originally considered in the search. The mass spectrum of such a model, excluded by the 1ℓ search, is shown in fig. 11.4(a).

The second category of models excluded comprises cases where the LSP is wino-like and nearly mass-degenerate with the chargino. These models correspond to the diagonal of the $m(\tilde{\chi}_1^\pm)$–$m(\tilde{\chi}_1^0)$ plane in fig. 11.2(a). As the mass difference between the LSP and the chargino is typically of the order of only a few 100 MeV, the chargino can become long-lived, and primarily decays to a LSP and an off-shell W boson that, in turn, decays into soft objects not reconstructed in the detector. If the chargino is produced with large momentum, it can live long enough to traverse multiple layers of the ATLAS pixel detector before decaying, leading to a disappearing track signature. Searches targeting prompt electroweakino decays are not expected to be sensitive to these models, and instead dedicated disappearing track searches are developed within the ATLAS Collaboration (cf. Ref. [300]). Even though no sensitivity to these models is expected from the 1ℓ search, a small set of models with a wino-like LSP can still be excluded. In these scenarios the next-to-lightest chargino $\tilde{\chi}_2^\pm$ is comparably light, such that the 1ℓ search is sensitive to $\tilde{\chi}_2^\pm\tilde{\chi}_2^0$ production with cross sections of $\mathcal{O}(1\,\text{fb})$. If the next-to-lightest chargino decays directly into the LSP via $\tilde{\chi}_2^\pm \to W^\pm\tilde{\chi}_1^0$, enough events with an isolated electron or muon can occur, allowing to exclude the model[§]. An exemplary mass spectrum of such a model, excluded by the 1ℓ search, is shown in fig. 11.4(b).

No sensitivity is observed for pMSSM models with higgsino-like electroweakinos, i.e. compressed mass spectra[‡]. This is expected, as the electroweakino decays in such scenarios typically produce off-shell W, Z and h bosons, resulting in very soft final state objects that the 1ℓ search is not optimised

[†] Figure C.3 illustrates this behaviour further.

[§] Provided that the branching fraction of the $\tilde{\chi}_2^0 \to h\tilde{\chi}_1^0$ decay is also large enough, such that a final state with a lepton, E_T^miss and two b-jets from a Higgs decay can be realised in a sufficient number of events.

[‡] The mass spectrum of an exemplary pMSSM model with higgsino-like LSP is shown in fig. C.5, highlighting that all three relevant electroweakinos ($\tilde{\chi}_1^\pm$, $\tilde{\chi}_2^0$ and $\tilde{\chi}_1^0$) are nearly mass-degenerate.

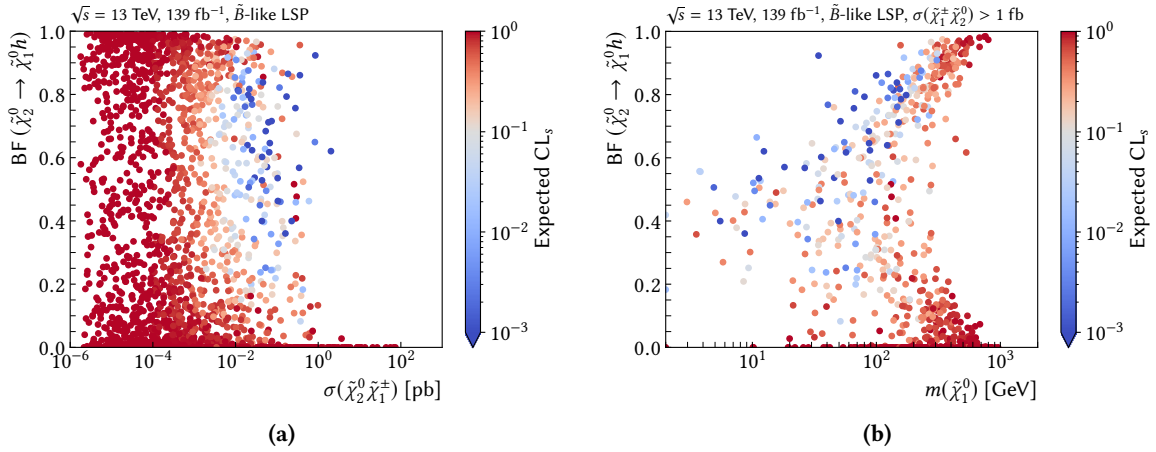

Figure 11.5: Density of the pMSSM models with bino-like $\tilde{\chi}_1^0$ projected onto the plane spanned by (a) the $\tilde{\chi}_1^\pm\tilde{\chi}_2^0$ pair production cross section and BF($\tilde{\chi}_2^0 \to h\tilde{\chi}_1^0$), and (b) $m(\tilde{\chi}_1^0)$ and BF($\tilde{\chi}_2^0 \to h\tilde{\chi}_1^0$). The expected CL$_s$ value obtained for each model using the 1ℓ search is colour-encoded. While models with a red tint are not expected to be excluded, models with a neutral white tint are on the boundary of expected exclusion, and models with a blue tint are expected to be excluded. Only models with a bino-like LSP are shown in both figures. In fig. (b), models are also required to satisfy $\sigma(\tilde{\chi}_1^\pm\tilde{\chi}_2^0) > 1$ fb.

for. Dedicated searches (as for example Ref. [91]) are being performed by the ATLAS Collaboration to target such compressed scenarios. Work is ongoing to include these searches in the large-scale scans of the pMSSM that the efforts discussed herein are embedded in.

In general, the sensitivity of the 1ℓ search to pMSSM models is significantly reduced, compared to the simplified model scenario, even in the electroweakino mass regions covered by the simplified model contour. The loss in sensitivity can be attributed to the fact that the simplified model assumes branching fractions of 100% of the $\tilde{\chi}_1^\pm \to W^\pm\tilde{\chi}_1^0$ and $\tilde{\chi}_2^0 \to h\tilde{\chi}_1^0$ decays (with on-shell W and h bosons). The decay of the chargino through an on-shell W boson is, in general, a good assumption in R-parity conserving models with $m(\tilde{\chi}_1^\pm) \gtrsim m(\tilde{\chi}_1^0) + m(W)$ and where the sleptons and charged and pseudoscalar Higgs bosons are heavier than the charginos and neutralinos. The decay of the next-to-lightest neutralino through a Higgs boson, however, turns out not to be the most probable decay mode in many models where the competing decay $\tilde{\chi}_2^0 \to Z\tilde{\chi}_1^0$ dominates instead. The couplings of the next-to-lightest neutralino to the Higgs boson are suppressed by powers of $|\mu|/M_2$ in the gaugino-like regions [301], meaning that the branching fraction of the $\tilde{\chi}_2^0 \to h\tilde{\chi}_1^0$ decay takes on reasonably high values only in models with an LSP containing a substantial bino component[†].

In the bulk of the $\tilde{\chi}_1^\pm$–$\tilde{\chi}_1^0$ plane (cf. fig. 11.2(a)) that mostly contains models with a bino-like LSP, many models cannot be excluded simply due to their relatively high $\tilde{\chi}_1^\pm/\tilde{\chi}_2^0$ masses, and thus low $\tilde{\chi}_1^\pm\tilde{\chi}_2^0$ pair production cross sections. Figure 11.5(a) shows a projection of the pMSSM models in a two-dimensional plane spanned by the $\tilde{\chi}_1^\pm\tilde{\chi}_2^0$ pair production cross section and BF($\tilde{\chi}_2^0 \to h\tilde{\chi}_1^0$). The colour of each model point indicates the expected CL$_s$ value[§], revealing that the 1ℓ search only starts to become sensitive to models with $\sigma(\tilde{\chi}_1^\pm\tilde{\chi}_2^0)$ larger than $\mathcal{O}(1\,\text{fb})$. This is in line with the sensitivity of the 1ℓ analysis obtained in the simplified model scenario, where model points with electroweakino pair

[†] The Higgs coupling suppression is illustrated in fig. C.4.

[§] The expected CL$_s$ is preferred here over the observed one as it provides a better overview of the sensitivity of the 1ℓ search.

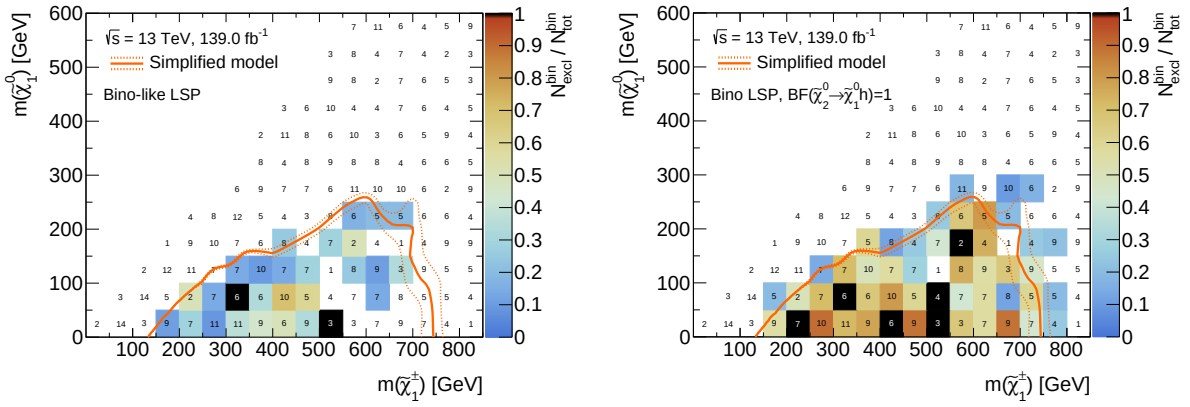

(a) Mixed BFs

(b) BF($\tilde{\chi}_2^0 \to h\tilde{\chi}_1^0$) = 1

Figure 11.6: Bin-by-bin fraction of excluded models with a bino-like $\tilde{\chi}_1^0$ as a function of $m(\tilde{\chi}_1^\pm)$ and $m(\tilde{\chi}_1^0)$. In fig. (a) the pMSSM models originally sampled are shown. In fig (b), the branching fraction of the $\tilde{\chi}_2^0 \to h\tilde{\chi}_1^0$ decay is manually set to 100% after which event generation and 1ℓ analysis evaluation are re-exectued. Only models with a bino-like LSP are shown in both figures.

production cross sections as low as 4.1 fb were expected to be excluded. Figure 11.5(a) moreover shows that, for many models with $\sigma(\tilde{\chi}_1^\pm \tilde{\chi}_2^0) \gtrsim 1$ fb, the branching fraction of the next-to-lightest neutralino decay via a Higgs boson is vanishingly small. This ultimately results in a low number of events with Higgs boson candidates, causing a lack of sensitivity in the context of the 1ℓ search.

Even with a sufficiently large electroweakino pair production cross section and at least moderate BF($\tilde{\chi}_2^0 \to h\tilde{\chi}_1^0$), a sizeable fraction of models turn out to have a relatively high LSP mass of more than 300 GeV, as shown in fig. 11.5(b). Coupled with an upper bound on the $\tilde{\chi}_1^\pm/\tilde{\chi}_2^0$ masses due to the pair production cross section requirement, these models thus tend to have comparably small electroweakino mass differences, resulting in signatures with reduced amounts of $E_\mathrm{T}^\mathrm{miss}$ and softer objects that may not always be reconstructed in the 1ℓ search and therefore contribute to a reduced sensitivity[†].

To illustrate the size of the sensitivity loss due to mixed branching fractions, a sizeable fraction of the models with a bino-like LSP have been reprocessed with BF($\tilde{\chi}_2^0 \to h\tilde{\chi}_1^0$) fixed to unity, and BF($\tilde{\chi}_2^0 \to Z\tilde{\chi}_1^0$) consequently set to disappear. The modified models were subsequently reanalysed with the 1ℓ search. Figure 11.6(b) reveals that significantly more pMSSM models can be excluded within the simplified model contour when the branching fraction assumptions of the simplified model are restored. As the $\tilde{\chi}_2^0$ decay into a Z boson and $\tilde{\chi}_1^0$ is the competing decay to $\tilde{\chi}_2^0 \to h\tilde{\chi}_1^0$, statistically combining searches targeting these decay modes could therefore recover the loss in sensitivity originating from mixed branching fractions in realistic SUSY models. Likewise, the development of searches targeting both decay modes at the same time, would also recover the full sensitivity[§].

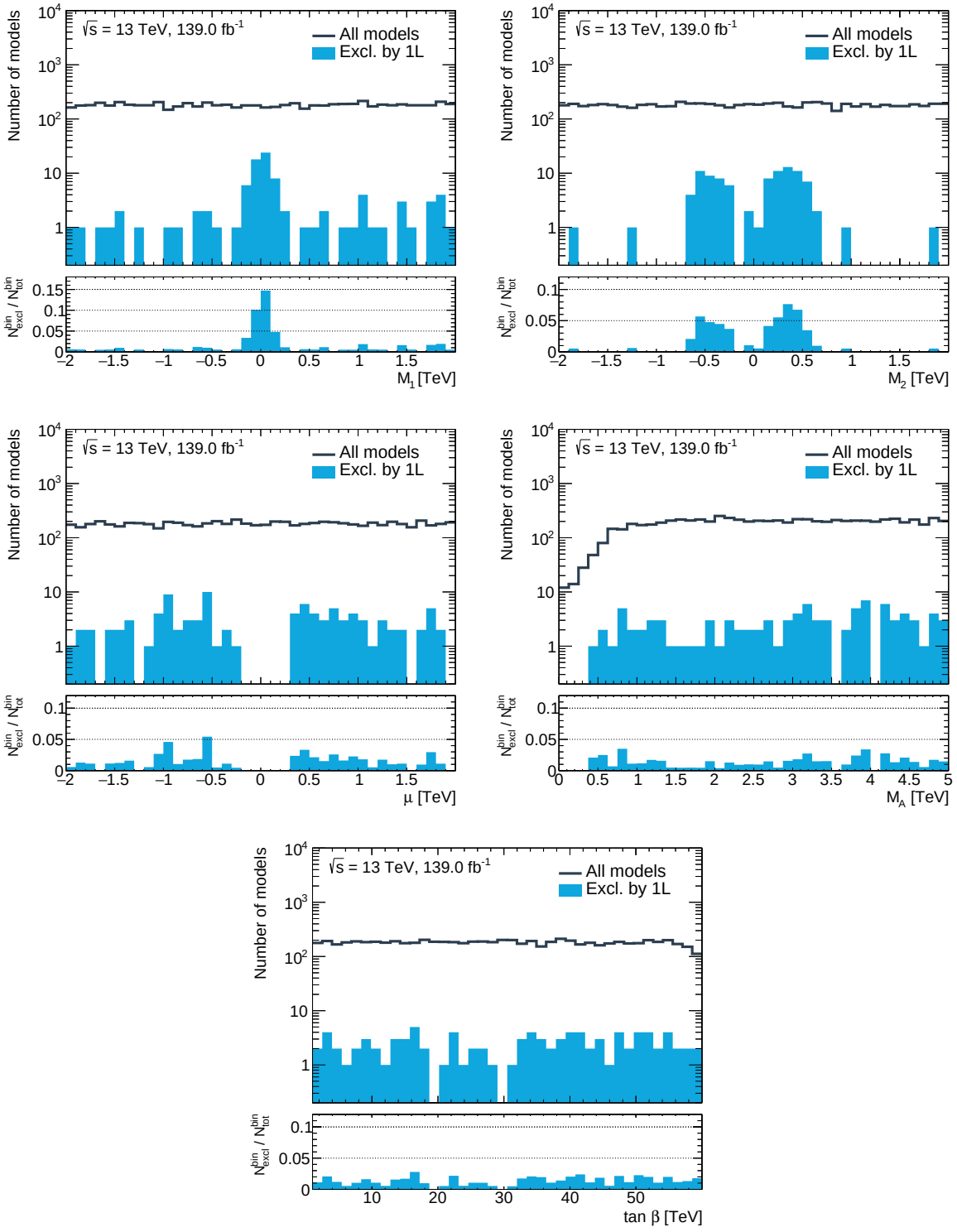

Figure 11.7: Bin-by-bin number of excluded models as a one-dimensional function of the pMSSM parameters relevant to the electroweak sector. The bin-wise fraction of excluded models, $N^{\text{bin}}_{\text{excl}}/N^{\text{bin}}_{\text{total}}$, is shown in the lower pad. All models are evaluated using the simplified likelihood of the 1ℓ search.

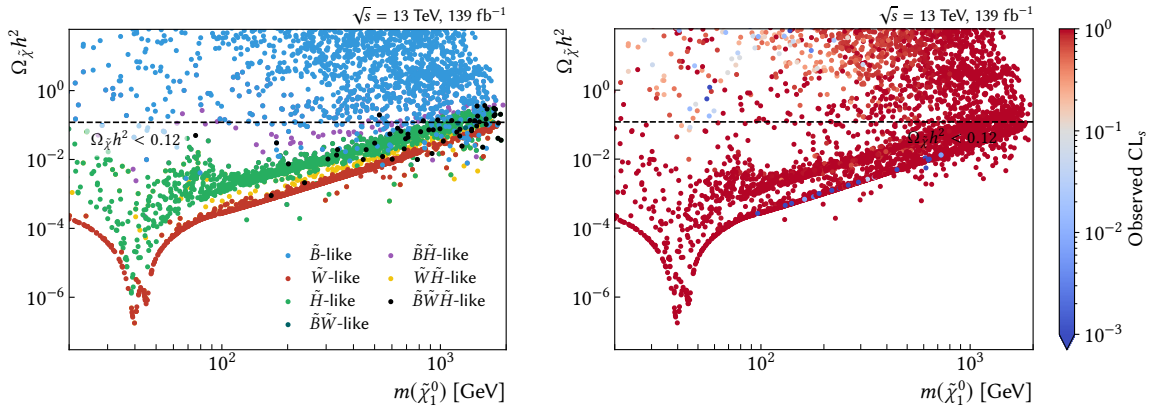

(a) **(b)**

Figure 11.8: Density of the pMSSM model points sampled in the plane spanned by the relic density and mass of the lightest neutralino. The model points are additionally shown as a function of (a) the nature of the LSP and (b) the observed CL$_s$ value obtained for 139 fb^{-1} of data using the 1ℓ search. The horizontal dashed line represents the DM relic density measurement by the Planck Collaboration [47], interpreted as an upper limit, $\Omega_{\tilde{\chi}}h^2 < 0.12$, such that the lightest neutralino can be a sub-dominant DM component.

11.4.2 Impact on pMSSM parameters

The impact of the 1ℓ search on the pMSSM parameters relevant to the electroweak sector are shown in one-dimensional distributions in fig. 11.7. As already discussed in section 11.4.1, the 1ℓ search has the largest impact for small values in the bino mass parameter M_1, leading to models with a bino-like LSP when M_1 is significantly smaller than M_2 and μ. Consequently, the proportion of excluded models peaks at slightly higher values in the distribution of the wino mass parameter, i.e. at around $|M_2| \approx 400$ GeV. As the search is not sensitive to compressed scenarios with a higgsino-like LSP, no models with small values in $|\mu|$ can be excluded.

Since the pseudoscalar Higgs boson does not directly enter the phenomenology of the models targeted by the 1ℓ search, only indirect constraints can be set on m_A, excluding models across the full range of the m_A distribution sampled. A similar behaviour is observed in $\tan\beta$ where the excluded models have values of $\tan\beta$ spanning the full range from 1 to 60. Likewise, no direct constraints on the trilinear scalar couplings (A_t, A_b, A_τ), and the remaining gluino and third generation squark mass parameters (M_3, $m_{\tilde{Q}_3}$, $m_{\tilde{u}_3}$, $m_{\tilde{d}_3}$) is observed[†].

11.4.3 Impact on dark matter relic density

The cosmological abundance of the lightest neutralino $\Omega_{\tilde{\chi}}h^2$ as a function of its type and mass is shown in fig. 11.8(a). The value of the dark matter (DM) relic density measured by the Planck Collaboration is also given [47]. The Planck measurement is interpreted as an upper limit on the DM relic density, thus allowing the $\tilde{\chi}_1^0$ to be a sub-dominant DM component.

† See fig. A.1 for an illustration of this kinematic effect.

§ Provided that they are targeted with statistically independent signal regions such that a combined likelihood can be built.

† Illustrated in fig. C.6.

Some interesting features are worth highlighting in fig. 11.8(a). First, most of the models sampled with a bino-like $\tilde{\chi}_1^0$ overproduce DM and result in a cosmological abundance that is too high. Of the pMSSM models sampled herein, only models with a $\tilde{\chi}_1^0$ containing a considerable wino or higgsino component consistently satisfy $\Omega_{\tilde{\chi}} h^2 < 0.12$ over a large range of the neutralino mass. Models with $m(\tilde{\chi}_1^0) \simeq m(Z)/2$ can produce especially low values in $\Omega_{\tilde{\chi}} h^2$ as the neutralino can resonantly annihilate through s-channel Z exchange. This is the so-called *Z-funnel*, a mechanism that becomes more efficient, the larger the higgsino component of the lightest neutralino is [302]. Likewise, models with a nearly mass-degenerate $\tilde{\chi}_1^\pm \tilde{\chi}_1^0$ pair with $m(\tilde{\chi}_1^\pm/\tilde{\chi}_2^0) \simeq m(W)/2$ can also produce low relic densities because of $\tilde{\chi}_1^\pm \tilde{\chi}_1^0$ co-annihilation through s-channel W exchange. A funnel similar to the Z-funnel, but involving s-channel Higgs exchange, exists at $m(\tilde{\chi}_1^0) \simeq m(h)/2$. It requires the $\tilde{\chi}_1^0$ to have a sizeable bino component [302] and is not visible in fig. 11.8(a) because models with a bino-like LSP are underrepresented in the relevant mass range.

In practice, the LEP limits[†] on the chargino mass of $m(\tilde{\chi}_1^\pm) > 92\,\text{GeV}$ [90] rule out models with $|M_2| \lesssim 100\,\text{GeV}$ and $|\mu| \lesssim 100\,\text{GeV}$, leaving only models with a bino-like LSP in the region with $m(\tilde{\chi}_1^0) \lesssim 100\,\text{GeV}$. Although models with a bino-like LSP could theoretically produce low $\tilde{\chi}_1^0$ relic density values through the Z- and h-funnels, in practice, such models are not sampled herein due to the sampling technique employed. To further study the impact of the 1ℓ search on models relevant to the DM phenomenology, i.e. models with a bino-like LSP in the Z- and h-funnels, a different sampling technique would need to be employed, including experimental constraints in the sampling priors in addition to specifically oversampling models with a bino-like LSP in the relevant mass range.

Although of limited use due to the limited number of models in the relevant parameter space, the impact of the 1ℓ search on the DM relic density can still be investigated with the models available. Figure 11.8(b) shows the $\tilde{\chi}_1^0$ cosmological abundance in dependence of the $\tilde{\chi}_1^0$ mass. Instead of encoding the nature of the $\tilde{\chi}_1^0$, the colour now encodes the observed CL_s value obtained by the 1ℓ search. By comparing with fig. 11.8(a), it can be seen that the majority of bino-like models excluded by the 1ℓ search overproduce DM. Through its limited sensitivity to some of the models with a wino-like $\tilde{\chi}_1^0$, the 1ℓ search is, however, still able to exclude some models with a compatible relic density.

11.5 Discussion

Large-scale reinterpretations in high-dimensional SUSY model spaces are crucial in order to assess the sensitivity of SUSY searches in the context of realistic SUSY scenarios. The evaluation of signal models at smeared truth-level, in combination with the simplified likelihoods introduced in chapter 10, offers a computationally efficient and reliable approach for such reinterpretations.

A reinterpretation of the 1ℓ search in a limited number of models sampled from the pMSSM with a focus on the electroweak sector has been discussed. It revealed that the 1ℓ search is sensitive to SUSY scenarios beyond the canonical simplified model originally considered. Although with some caveats, the simplified model phenomenology generally maps reasonably well onto a portion of the pMSSM parameter space. The 1ℓ search is, as expected, found to be most sensitive to pMSSM models with wino-like $\tilde{\chi}_1^\pm \tilde{\chi}_2^0$ pair production and a bino-like LSP. Interestingly, some sensitivity was found towards $\tilde{\chi}_2^\pm \tilde{\chi}_2^0$ pair production in models with a wino-like LSP.

[†] The limit on the chargino mass of $m(\tilde{\chi}_1^\pm) > 92\,\text{GeV}$ considered herein is a conservative lower limit. In a large region of the phase space, the limits on the chargino mass set by LEP reach as high as 103.5 GeV. The impact of the chargino mass limit in the $\Omega_{\tilde{\chi}} h^2$–$m(\tilde{\chi}_1^0)$ projection is shown in fig. C.7.

In general, the sensitivity of the 1ℓ search towards pMSSM models is observed to be negatively impacted by the competing decays $\tilde{\chi}_2^0 \to Z\tilde{\chi}_1^0$ and $\tilde{\chi}_2^0 \to h\tilde{\chi}_1^0$, breaking one of the main assumptions of the simplified model. In order to maximise the sensitivity of future searches to $\tilde{\chi}_1^\pm\tilde{\chi}_2^0$ pair production in more complete SUSY scenarios, it is therefore crucial to target both decay modes at the same time. In searches targeting final states with a lepton, multiple jets and missing transverse momentum, both the b-jet multiplicity as well as the invariant mass of the jets originating from the decays $h \to b\bar{b}$ and $Z \to q\bar{q}$ can easily be exploited to develop disjoint[†] signal regions targeting both decay modes.

Beyond the combination of single decay modes, it could be worth targeting not only $\tilde{\chi}_1^\pm\tilde{\chi}_2^0$ pair production, but also $\tilde{\chi}_1^\pm\tilde{\chi}_1^\pm$ pair production at the same time in a single likelihood function. In the ATLAS Collaboration, work is for example ongoing to perform a search for electroweakinos in the 1ℓ final state using dedicated signal regions simultaneously targeting both $\tilde{\chi}_1^\pm\tilde{\chi}_2^0 \to WZ\tilde{\chi}_1^0\tilde{\chi}_1^0$ and $\tilde{\chi}_1^\pm\tilde{\chi}_1^\pm \to WW\tilde{\chi}_1^0\tilde{\chi}_1^0$.

Finally, the impact of the 1ℓ search on the DM relic density was discussed. The parameter ranges and sampling technique chosen were used to allow the scan to be as general as possible. For this reason, a large fraction of the models sampled are not directly relevant to the DM phenomenology. Only a small number of models with a bino-like $\tilde{\chi}_1^0$ are sampled from the Z- and h-funnel region where $\Omega_{\tilde{\chi}}h^2 < 0.12$ can be expected to be satisfied for a sizeable fraction of such models. Outside of these two funnels, models with a bino-like $\tilde{\chi}_1^0$ satisfying the relic density constraint tend to have a $\tilde{\chi}_1^0$ mass outside of the range that the 1ℓ search is sensitive to.

In order to be able to further investigate the impact of the 1ℓ search on DM observables, a different sampling technique would need to be adopted, including experimental constraints in the sampling priors and oversampling the relevant regions of the parameter space. The initial sampling of the models, the calculation of their mass spectra and other observables, and the application of experimental constraints is computationally relatively cheap. Therefore, oversampling the relevant parameter space with a brute-force method can be a feasible approach. Machine learning approaches, as for example clustering techniques, can additionally be used to group models into different phenomenological *clusters*, possibly allowing to determine refined parameter ranges to be manually oversampled. Alternatively, active *smart sampling* approaches (as opposed to manually determining and oversampling certain parameter ranges) relying on machine learning methods can be leveraged and are being studied with the aim of improving the sampling efficiency. For example, to dynamically oversample regions of the parameter space with rapidly changing phenomenology and, conversely, undersample regions with low experimental sensitivity or only slowly changing phenomenology[§], information geometry methods [304] relying on the Fisher information matrix could be exploited [305].

[†] Building signal regions that are not orthogonal to each other prevents the construction of a combined likelihood and thus does not allow full statistical combination.

[§] The formalisation of this problem is in many aspects directly related to the problem of finding an *inverse map* from the space of LHC signatures to the parameter space of beyond the Standard Model (BSM) models, discussed in Ref. [303].

Part IV

Summary and Outlook

Part V

Appendices

Appendix C

Reinterpretation in the pMSSM

The following sections provide supporting material for the reinterpretation of the 1ℓ search in the pMSSM, discussed in chapter 11.

C.1 Further validation of the simplified likelihood

Figure C.1 compares the observed CL_s values obtained for the pMSSM models sampled using the various likelihoods of the 1ℓ search discussed throughout part III of this thesis. In general, the observed CL_s values from the simplified likelihood are closer to those obtained using the full likelihood, than the ones obtained using the single-bin likelihood (built using the discovery signal regions).

Although revealing a good agreement, the CL_s values naturally do not exactly match. For this reason, the simplified likelihood can only be used for models giving observed CL_s moderately far away from the exclusion boundary at 0.05. Models with a CL_s value too close to 0.05 need to be evaluated using the full likelihood and RECAST for full statistical precision. Compared to the single-bin approach using the discovery signal regions, the benefit of the simplified likelihood is that, due to the improved agreement in observed CL_s, the interval around $CL_s = 0.05$ defining models to be evaluated using the full likelihood can be chosen to be significantly narrower. Ultimately, this approach does allows for more efficient pMSSM scans where a smaller fraction of models needs to be evaluated at full precision.

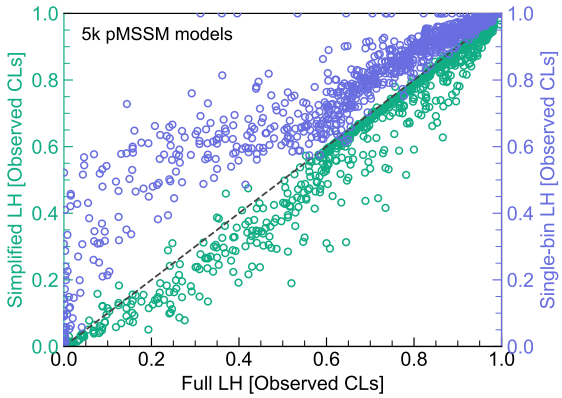

Figure C.1: Observed CL_s values obtained for all pMSSM models sampled for different likelihood configurations of the 1ℓ search. In green, the simplified likelihood discussed in chapter 10 is compared with the full analysis likelihood. In purple, the single-bin likelihood configuration using the discovery signal regions is compared with the full likelihood.

C.2 Phenomenology of the LSP

Figure C.2 shows the LSP type as a function of the pMSSM parameters M_1, M_2, μ and $\tan\beta$. Models with $|M_1| \ll |M_2|, |\mu|$ tend to have an LSP with dominant bino component, while models with $|M_2| \ll |M_1|, |\mu|$, have an LSP that is mostly wino-like. Similarly, models with $|\mu| \ll |M_1|, |M_2|$ have mostly higgsino-like LSPs. The parameter $\tan\beta$ does not have a large impact on the LSP type within the ranges sampled.

Figure C.3 shows the fraction of models excluded by the 1ℓ search in different two-dimensional projections on the electroweakino masses. Models with a bino-like LSP tend to have nearly mass-degenerate $\tilde{\chi}_1^\pm$ and $\tilde{\chi}_2^0$ and are thus close to the canonical simplified model considered in the search. Models with a wino-like LSP have nearly mass-degenerate $\tilde{\chi}_1^\pm$ and $\tilde{\chi}_1^0$. In such models, the 1ℓ search can be sensitive to $\tilde{\chi}_2^\pm \tilde{\chi}_2^0$ production.

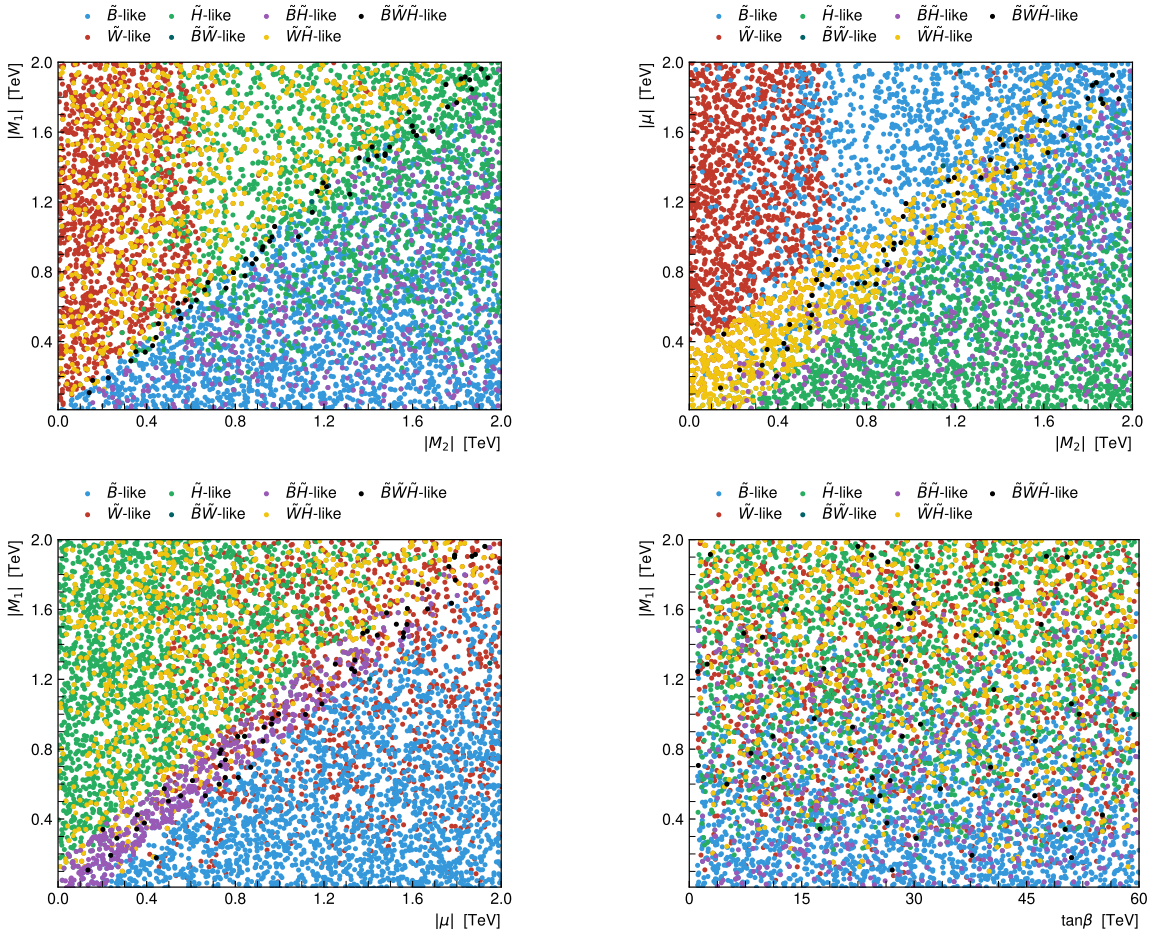

Figure C.2: Phenomenology of the LSP as a function of two-dimensional projections of the pMSSM parameter space. Each point in the plots corresponds to a unique pMSSM model sampled. The colour codes the nature of the LSP using the definitions introduced in section 11.3.

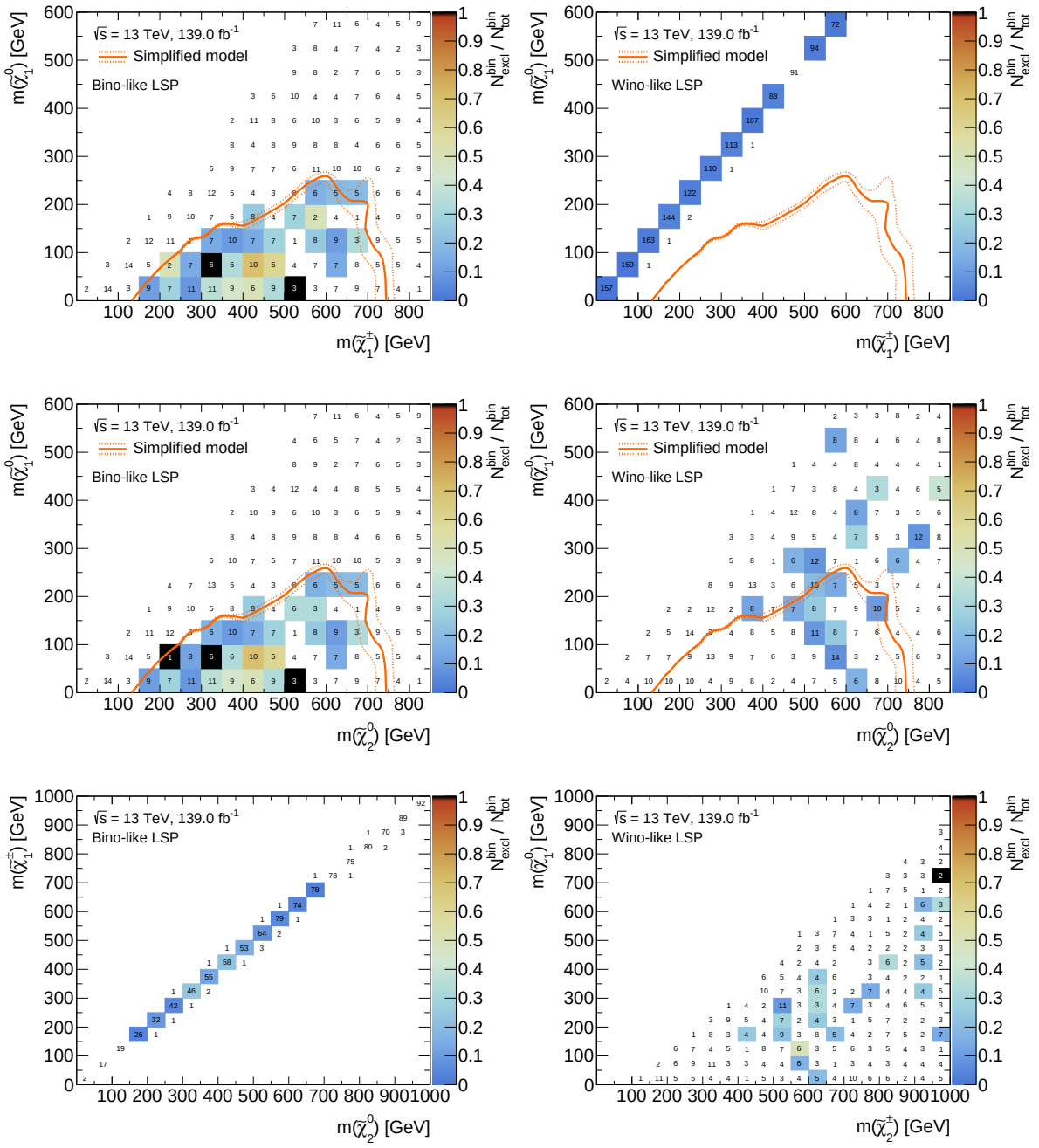

Figure C.3: Bin-by-bin fraction of excluded models as a two-dimensional function of the relevant sparticle masses. Only pMSSM models with a bino-like (wino-like) LSP are shown on the left (right). The numbers in the bins correspond to the total number of models sampled falling into the respective bin. The bin-wise fraction of models excluded by the 1ℓ search is encoded with a colour bar ranging from 0 to 1. Where all models in a given bin are excluded, the bin is coloured in black. Bins without any models excluded are left white. Models are evaluated using the simplified likelihood of the 1ℓ search. If applicable, the simplified model contour is shown in orange.

C.3 Model properties

As illustrated in fig. C.4, the couplings of the $\tilde{\chi}_2^0$ to the Higgs boson are suppressed by powers of $|\mu|/M_2$ in the wino-like and bino-like scenarios [301], meaning that the branching fraction of $\tilde{\chi}_2^0 \rightarrow h\tilde{\chi}_1^0$ takes on reasonably high values only in models with an LSP that is nearly pure bino.

Figure C.5 shows the compressed mass spectrum of an exemplary pMSSM model point with higgsino-like $\tilde{\chi}_1^0$, a model that the 1ℓ search is not expected to be sensitive to.

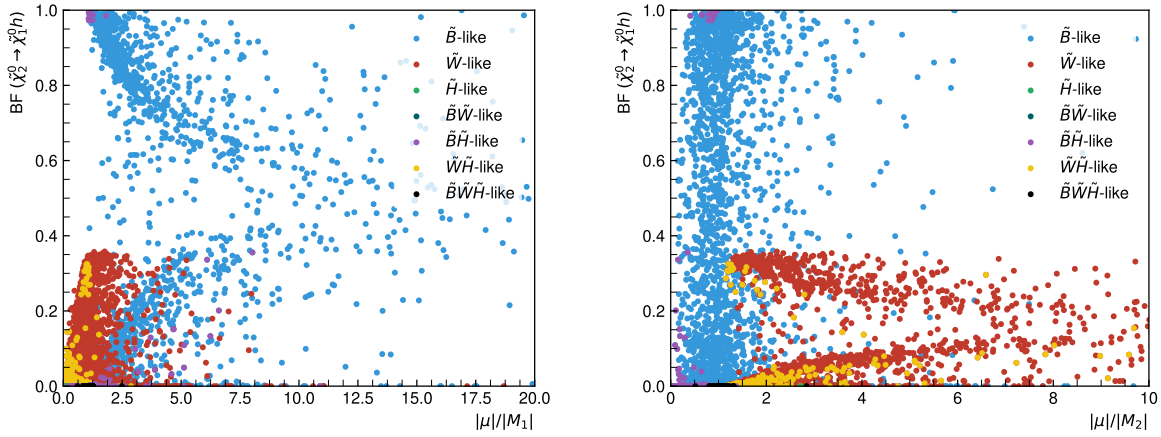

(a) **(b)**

Figure C.4: Density of the pMSSM models projected onto the plane spanned by BF($\tilde{\chi}_2^0 \rightarrow h\tilde{\chi}_1^0$) and (a) $|\mu|/|M_1|$ or (b) $|\mu|/|M_2|$. Models are shown as a function of their $\tilde{\chi}_1^0$ type.

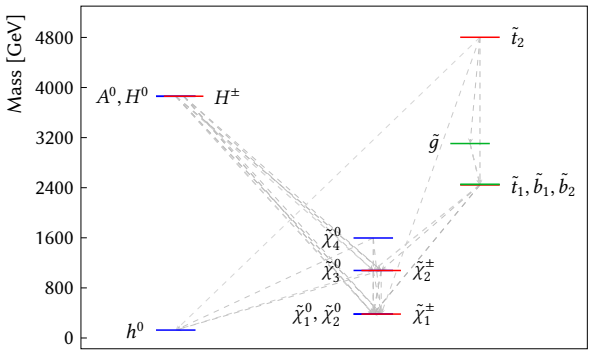

Figure C.5: Mass spectrum of an exemplary pMSSM model with higgsino like lightest electroweakinos. The branching fractions of the different decays are indicated through the width and and greyscale colour (pure black being 100%, pure white being 0%) of the arrows. Branching fractions below 10% are suppressed for the sake of visibility. Figure generated using `pyslha` [92].

C.4 Impact of the 1ℓ search on the pMSSM parameters

In fig. C.6, the impact of the 1ℓ search on the reminaing pMSSM parameters sampled, not already shown in section 11.4.2, are provided. As before, the full set of models evaluated with the 1ℓ search is shown as black line, while the bin-wise number of models excluded by the search are indicated with the blue histogram. An additional pad indicates the bin-wise fraction of models excluded.

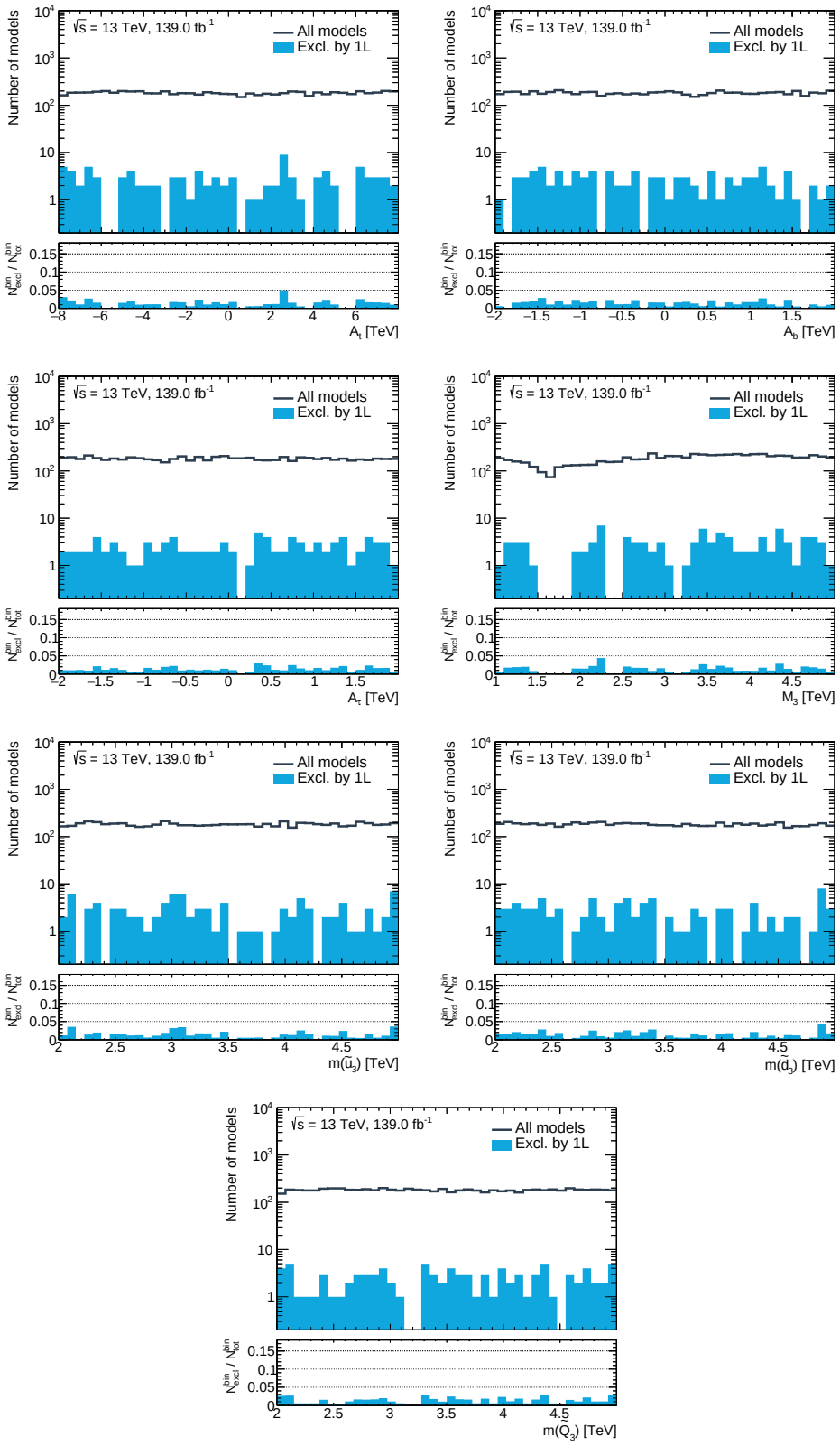

Figure C.6: Bin-by-bin number of excluded models as a one-dimensional function of the remaining pMSSM parameters not already shown in fig. 11.7. The bin-wise fraction of excluded models, $N^{\text{bin}}_{\text{excl}}/N^{\text{bin}}_{\text{total}}$, is shown in the lower pad. All models are evaluated using the simplified likelihood of the 1ℓ search.

C.5 Impact of the 1ℓ search on the dark matter relic density

Figure C.7 compares the density of pMSSM models in a two-dimensional projection on the $\Omega_{\tilde{\chi}}h^2$–$m(\tilde{\chi}_1^0)$ plane before and after the conservative LEP constraint on the chargino mass of $m(\tilde{\chi}_1^\pm) > 92\,\text{GeV}$ [90] is applied. Only models with a bino-like LSP provide a light LSP with mass below 10^2 GeV after the LEP constraint. In order for the Z- and h-funnels to become visible, i.e. for there to be a sizeable number of models with a light bino-like LSP and $\Omega_{\tilde{\chi}}h^2 < 0.12$, the region with $m(\tilde{\chi}_1^0) < 10^2$ GeV would need to be oversampled. Due to the lack thereof within the scope of this thesis, only a small number of such models are sampled and subsequently evaluated using the 1ℓ search.

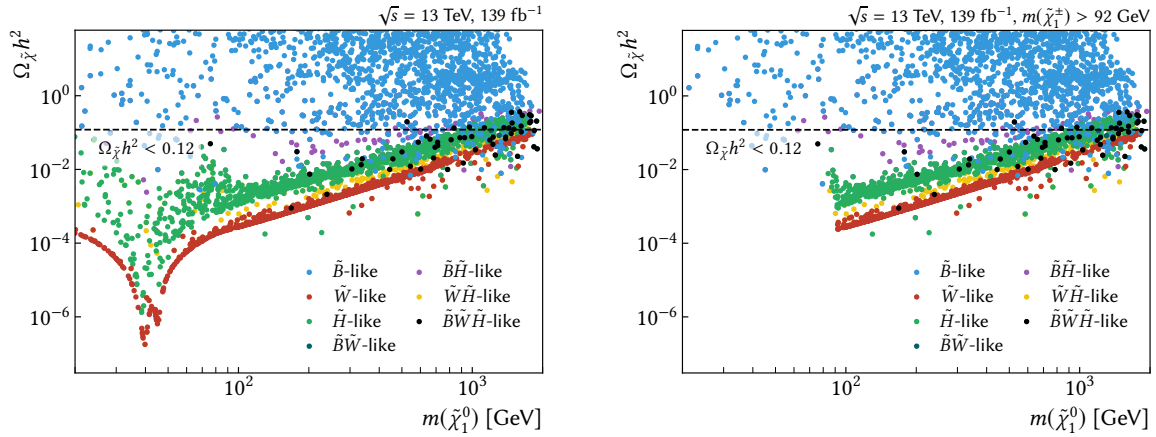

(a) Without LEP constraint

(b) With LEP constraint

Figure C.7: Density of the pMSSM model points sampled in the plane spanned by the relic density and the $\tilde{\chi}_1^0$ mass. The model points are additionally shown as a function of the nature of their $\tilde{\chi}_1^0$. In fig. (a) all pMSSM models originally sampled and evaluated are shown. In fig. (b), only models satisfying the constraint $m(\tilde{\chi}_1^\pm) > 92\,\text{GeV}$ set by LEP [90] are shown. The horizontal dashed line represents the DM relic density measurement by the Planck Collaboration, interpreted as an upper limit such that the $\tilde{\chi}_1^0$ can be a sub-dominant DM component.

Abbreviations

BSM beyond the Standard Model. 170

DM dark matter. 168–170, 204

LEP Large Electron Positron. 160, 169, 204

LHC Large Hadron Collider. 159, 170

LSP lightest supersymmetric particle. 159–162, 164–166, 168, 169, 200–202, 204

NLO next-to-leading order. 159

PDF parton distribution function. 160

pMSSM phenomenological Minimal Supersymmetric Standard Model. 157, 159–162, 164–170, 199–204

SM Standard Model. 159

SUSY Supersymmetry. 157, 159, 166, 169, 170

Bibliography

[1] ATLAS Collaboration, "Observation of a new particle in the search for the Standard Model Higgs boson with the ATLAS detector at the LHC," *Phys. Lett. B* **716** (2012) 1, arXiv:1207.7214 [hep-ex].

[2] CMS Collaboration, "Observation of a new boson at a mass of 125 GeV with the CMS experiment at the LHC," *Phys. Lett. B* **716** (2012) 30, arXiv:1207.7235 [hep-ex].

[3] I. C. Brock and T. Schorner-Sadenius, *Physics at the terascale*. Wiley, Weinheim, 2011. https://cds.cern.ch/record/1354959.

[4] M. E. Peskin and D. V. Schroeder, *An Introduction to quantum field theory*. Addison-Wesley, Reading, USA, 1995.

[5] S. P. Martin, "A Supersymmetry Primer," *Adv. Ser. Direct. High Energy Phys.* **18** (1998) 1, arXiv:hep-ph/9709356.

[6] M. Bustamante, L. Cieri, and J. Ellis, "Beyond the Standard Model for Montaneros," in *5th CERN - Latin American School of High-Energy Physics*. 11, 2009. arXiv:0911.4409 [hep-ph].

[7] L. Brown, *The Birth of particle physics*. Cambridge University Press, Cambridge, 1986.

[8] P. J. Mohr, D. B. Newell, and B. N. Taylor, "CODATA Recommended Values of the Fundamental Physical Constants: 2014," *Rev. Mod. Phys.* **88** no. 3, (2016) 035009, arXiv:1507.07956 [physics.atom-ph].

[9] Particle Data Group, "Review of Particle Physics," *Prog. Theor. Exp. Phys* **2020** no. 8, (08, 2020) .

[10] Super-Kamiokande Collaboration, "Evidence for oscillation of atmospheric neutrinos," *Phys. Rev. Lett.* **81** (1998) 1562–1567, arXiv:hep-ex/9807003.

[11] Z. Maki, M. Nakagawa, and S. Sakata, "Remarks on the unified model of elementary particles," *Prog. Theor. Phys.* **28** (1962) 870–880.

[12] N. Cabibbo, "Unitary Symmetry and Leptonic Decays," *Phys. Rev. Lett.* **10** (1963) 531–533.

[13] M. Kobayashi and T. Maskawa, "CP Violation in the Renormalizable Theory of Weak Interaction," *Prog. Theor. Phys.* **49** (1973) 652–657.

[14] E. Noether, "Invariant Variation Problems," *Gott. Nachr.* **1918** (1918) 235–257, arXiv:physics/0503066.

[15] J. C. Ward, "An Identity in Quantum Electrodynamics," *Phys. Rev.* **78** (1950) 182.

[16] Y. Takahashi, "On the generalized ward identity," *Il Nuovo Cimento (1955-1965)* **6** no. 2, (1957) 371–375.

[17] G. 't Hooft, "Renormalization of Massless Yang-Mills Fields," *Nucl. Phys. B* **33** (1971) 173–199.

[18] J. C. Taylor, "Ward Identities and Charge Renormalization of the Yang-Mills Field," *Nucl. Phys. B* **33** (1971) 436–444.

[19] A. A. Slavnov, "Ward Identities in Gauge Theories," *Theor. Math. Phys.* **10** (1972) 99–107.

[20] C.-N. Yang and R. L. Mills, "Conservation of Isotopic Spin and Isotopic Gauge Invariance," *Phys. Rev.* **96** (1954) 191–195.

[21] K. G. Wilson, "Confinement of Quarks," *Phys. Rev. D* **10** (1974) 2445–2459.

[22] T. DeGrand and C. DeTar, *Lattice Methods for Quantum Chromodynamics*. World Scientific, Singapore, 2006.

[23] S. L. Glashow, "Partial Symmetries of Weak Interactions," *Nucl. Phys.* **22** (1961) 579–588.

[24] S. Weinberg, "A Model of Leptons," *Phys. Rev. Lett.* **19** (1967) 1264–1266.

[25] A. Salam, "Weak and Electromagnetic Interactions," *Conf. Proc. C* **680519** (1968) 367–377.

[26] C. S. Wu, E. Ambler, R. W. Hayward, *et al.*, "Experimental Test of Parity Conservation in β Decay," *Phys. Rev.* **105** (1957) 1413–1414.

[27] M. Gell-Mann, "The interpretation of the new particles as displaced charge multiplets," *Nuovo Cim.* **4** no. S2, (1956) 848–866.

[28] K. Nishijima, "Charge Independence Theory of V Particles," *Prog. Theor. Phys.* **13** no. 3, (1955) 285–304.

[29] T. Nakano and K. Nishijima, "Charge Independence for V-particles," *Prog. Theor. Phys.* **10** (1953) 581–582.

[30] F. Englert and R. Brout, "Broken Symmetry and the Mass of Gauge Vector Mesons," *Phys. Rev. Lett.* **13** (1964) 321–323.

[31] P. W. Higgs, "Broken Symmetries and the Masses of Gauge Bosons," *Phys. Rev. Lett.* **13** (1964) 508–509.

[32] P. W. Higgs, "Spontaneous Symmetry Breakdown without Massless Bosons," *Phys. Rev.* **145** (1966) 1156–1163.

[33] Y. Nambu, "Quasiparticles and Gauge Invariance in the Theory of Superconductivity," *Phys. Rev.* **117** (1960) 648–663.

[34] J. Goldstone, "Field Theories with Superconductor Solutions," *Nuovo Cim.* **19** (1961) 154–164.

[35] V. Brdar, A. J. Helmboldt, S. Iwamoto, and K. Schmitz, "Type-I Seesaw as the Common Origin of Neutrino Mass, Baryon Asymmetry, and the Electroweak Scale," *Phys. Rev. D* **100** (2019) 075029, arXiv:1905.12634 [hep-ph].

[36] G. 't Hooft and M. J. G. Veltman, "Regularization and Renormalization of Gauge Fields," *Nucl. Phys. B* **44** (1972) 189–213.

[37] G. Kane and M. Shifman, *The supersymmetric world : the beginnings of the theory*. World Scientific, Singapore, 2000.

[38] F. Zwicky, "Die Rotverschiebung von extragalaktischen Nebeln," *Helv. Phys. Acta* **6** (1933) 110–127.

[39] V. C. Rubin and W. K. Ford, Jr., "Rotation of the Andromeda Nebula from a Spectroscopic Survey of Emission Regions," *Astrophys. J.* **159** (1970) 379–403.

[40] G. Bertone, D. Hooper, and J. Silk, "Particle dark matter: Evidence, candidates and constraints," *Phys. Rept.* **405** (2005) 279–390, arXiv:hep-ph/0404175.

[41] D. Clowe, M. Bradac, A. H. Gonzalez, *et al.*, "A direct empirical proof of the existence of dark matter," *Astrophys. J.* **648** (2006) L109–L113, arXiv:astro-ph/0608407.

[42] A. Taylor, S. Dye, T. J. Broadhurst, *et al.*, "Gravitational lens magnification and the mass of abell 1689," *Astrophys. J.* **501** (1998) 539, arXiv:astro-ph/9801158.

[43] C. L. Bennett, A. Banday, K. M. Gorski, *et al.*, "Four year COBE DMR cosmic microwave background observations: Maps and basic results," *Astrophys. J. Lett.* **464** (1996) L1–L4, arXiv:astro-ph/9601067.

[44] COBE Collaboration, "Structure in the COBE differential microwave radiometer first year maps," *Astrophys. J. Lett.* **396** (1992) L1–L5.

[45] WMAP Collaboration, C. L. Bennett *et al.*, "Nine-Year Wilkinson Microwave Anisotropy Probe (WMAP) Observations: Final Maps and Results," *Astrophys. J. Suppl.* **208** (2013) 20, arXiv:1212.5225 [astro-ph.CO].

[46] WMAP Collaboration, G. Hinshaw *et al.*, "Nine-Year Wilkinson Microwave Anisotropy Probe (WMAP) Observations: Cosmological Parameter Results," *Astrophys. J. Suppl.* **208** (2013) 19, arXiv:1212.5226 [astro-ph.CO].

[47] Planck Collaboration, "Planck 2018 results. I. Overview and the cosmological legacy of Planck," *Astron. Astrophys.* **641** (2020) A1, arXiv:1807.06205 [astro-ph.CO].

[48] A. Liddle, *An introduction to modern cosmology*. Wiley, Chichester, 3rd ed., Mar, 2015.

[49] Planck Collaboration, "Planck 2018 results. VI. Cosmological parameters," *Astron. Astrophys.* **641** (2020) A6, arXiv:1807.06209 [astro-ph.CO].

[50] H. Georgi and S. L. Glashow, "Unity of All Elementary Particle Forces," *Phys. Rev. Lett.* **32** (1974) 438–441.

[51] I. Aitchison, *Supersymmetry in Particle Physics. An Elementary Introduction*. Cambridge University Press, Cambridge, 2007.

[52] Muon g-2 Collaboration, "Final Report of the Muon E821 Anomalous Magnetic Moment Measurement at BNL," *Phys. Rev. D* **73** (2006) 072003, arXiv:hep-ex/0602035.

[53] H. Baer and X. Tata, *Weak Scale Supersymmetry: From Superfields to Scattering Events*. Cambridge University Press, Cambridge, 2006.

[54] T. Aoyama *et al.*, "The anomalous magnetic moment of the muon in the Standard Model," *Phys. Rept.* **887** (2020) 1–166, arXiv:2006.04822 [hep-ph].

[55] Muon g-2 Collaboration, "Measurement of the Positive Muon Anomalous Magnetic Moment to 0.46 ppm," *Phys. Rev. Lett.* **126** no. 14, (2021) 141801, arXiv:2104.03281 [hep-ex].

[56] A. Czarnecki and W. J. Marciano, "The Muon anomalous magnetic moment: A Harbinger for 'new physics'," *Phys. Rev. D* **64** (2001) 013014, arXiv:hep-ph/0102122.

[57] J. L. Feng and K. T. Matchev, "Supersymmetry and the anomalous magnetic moment of the muon," *Phys. Rev. Lett.* **86** (2001) 3480–3483, arXiv:hep-ph/0102146.

[58] S. R. Coleman and J. Mandula, "All Possible Symmetries of the S Matrix," *Phys. Rev.* **159** (1967) 1251–1256.

[59] R. Haag, J. T. Lopuszanski, and M. Sohnius, "All Possible Generators of Supersymmetries of the s Matrix," *Nucl. Phys. B* **88** (1975) 257.

[60] J. Wess and B. Zumino, "Supergauge transformations in four dimensions," *Nucl. Phys. B* **70** (1974) 39.

[61] H. Georgi and S. L. Glashow, "Gauge theories without anomalies," *Phys. Rev. D* **6** (1972) 429.

[62] S. Dimopoulos and D. W. Sutter, "The Supersymmetric flavor problem," *Nucl. Phys. B* **452** (1995) 496–512, arXiv:hep-ph/9504415.

[63] MEG Collaboration, "Final Results of the MEG Experiment," *Nuovo Cim. C* **39** no. 4, (2017) 325, arXiv:1606.08168 [hep-ex].

[64] H. P. Nilles, "Supersymmetry, Supergravity and Particle Physics," *Phys. Rept.* **110** (1984) 1–162.

[65] A. B. Lahanas and D. V. Nanopoulos, "The Road to No Scale Supergravity," *Phys. Rept.* **145** (1987) 1.

[66] J. L. Feng, A. Rajaraman, and F. Takayama, "Superweakly interacting massive particles," *Phys. Rev. Lett.* **91** (2003) 011302, arXiv:hep-ph/0302215.

[67] S. Y. Choi, J. Kalinowski, G. A. Moortgat-Pick, and P. M. Zerwas, "Analysis of the neutralino system in supersymmetric theories," *Eur. Phys. J. C* **22** (2001) 563–579, arXiv:hep-ph/0108117. [Addendum: Eur. Phys. J. C 23, 769–772 (2002)].

[68] Super-Kamiokande Collaboration, "Search for proton decay via $p \to e^+\pi^0$ and $p \to \mu^+\pi^0$ in 0.31 megaton-years exposure of the Super-Kamiokande water Cherenkov detector," *Phys. Rev. D* **95** no. 1, (2017) 012004, arXiv:1610.03597 [hep-ex].

[69] J. R. Ellis, "Beyond the standard model for hill walkers," in *1998 European School of High-Energy Physics*, pp. 133–196. 8, 1998. arXiv:hep-ph/9812235.

[70] J. R. Ellis, J. Hagelin, D. V. Nanopoulos, *et al.*, "Supersymmetric Relics from the Big Bang," *Nucl. Phys. B* **238** (1984) 453–476.

[71] D. O. Caldwell, R. M. Eisberg, D. M. Grumm, *et al.*, "Laboratory Limits on Galactic Cold Dark Matter," *Phys. Rev. Lett.* **61** (1988) 510.

[72] Kamiokande Collaboration, M. Mori *et al.*, "Search for neutralino dark matter in Kamiokande," *Phys. Rev. D* **48** (1993) 5505–5518.

[73] CDMS Collaboration, D. S. Akerib *et al.*, "Exclusion limits on the WIMP-nucleon cross section from the first run of the Cryogenic Dark Matter Search in the Soudan Underground Laboratory," *Phys. Rev. D* **72** (2005) 052009, arXiv:astro-ph/0507190.

[74] A. Djouadi, J.-L. Kneur, and G. Moultaka, "SuSpect: A Fortran code for the supersymmetric and Higgs particle spectrum in the MSSM," *Comput. Phys. Commun.* **176** (2007) 426–455, arXiv:hep-ph/0211331.

[75] C. F. Berger, J. S. Gainer, J. L. Hewett, and T. G. Rizzo, "Supersymmetry Without Prejudice," *JHEP* **02** (2009) 023, arXiv:0812.0980 [hep-ph].

[76] J. Alwall, P. Schuster, and N. Toro, "Simplified Models for a First Characterization of New Physics at the LHC," *Phys. Rev. D* **79** (2009) 075020, arXiv:0810.3921 [hep-ph].

[77] LHC New Physics Working Group, "Simplified Models for LHC New Physics Searches," *J. Phys. G* **39** (2012) 105005, arXiv:1105.2838 [hep-ph].

[78] D. S. Alves, E. Izaguirre, and J. G. Wacker, "Where the Sidewalk Ends: Jets and Missing Energy Search Strategies for the 7 TeV LHC," *JHEP* **10** (2011) 012, arXiv:1102.5338 [hep-ph].

[79] F. Ambrogi, S. Kraml, S. Kulkarni, *et al.*, "On the coverage of the pMSSM by simplified model results," *Eur. Phys. J. C* **78** no. 3, (2018) 215, arXiv:1707.09036 [hep-ph].

[80] O. Buchmueller and J. Marrouche, "Universal mass limits on gluino and third-generation squarks in the context of Natural-like SUSY spectra," *Int. J. Mod. Phys. A* **29** no. 06, (2014) 1450032, arXiv:1304.2185 [hep-ph].

[81] W. Beenakker, C. Borschensky, M. Krämer, *et al.*, "NNLL-fast: predictions for coloured supersymmetric particle production at the LHC with threshold and Coulomb resummation," *JHEP* **12** (2016) 133, arXiv:1607.07741 [hep-ph].

[82] M. Beneke, M. Czakon, P. Falgari, *et al.*, "Threshold expansion of the $gg(q\bar{q}) \to Q\bar{Q} + X$ cross section at $\mathcal{O}(\alpha_s^4)$," *Phys. Lett. B* **690** (2010) 483, arXiv:0911.5166 [hep-ph].

[83] J. Fiaschi and M. Klasen, "Neutralino-chargino pair production at NLO+NLL with resummation-improved parton density functions for LHC Run II," *Phys. Rev. D* **98** no. 5, (2018) 055014, arXiv:1805.11322 [hep-ph].

[84] B. Fuks, M. Klasen, D. R. Lamprea, and M. Rothering, "Gaugino production in proton-proton collisions at a center-of-mass energy of 8 TeV," *JHEP* **10** (2012) 081, arXiv:1207.2159 [hep-ph].

[85] J. Fiaschi and M. Klasen, "Slepton pair production at the LHC in NLO+NLL with resummation-improved parton densities," *JHEP* **03** (2018) 094, arXiv:1801.10357 [hep-ph].

[86] ATLAS Collaboration, "Dark matter interpretations of ATLAS searches for the electroweak production of supersymmetric particles in $\sqrt{s} = 8$ TeV proton-proton collisions," *JHEP* **09** (2016) 175, arXiv:1608.00872 [hep-ex].

[87] ATLAS Collaboration, "Summary of the ATLAS experiment's sensitivity to supersymmetry after LHC Run 1 — interpreted in the phenomenological MSSM," *JHEP* **10** (2015) 134, arXiv:1508.06608 [hep-ex].

[88] ATLAS Collaboration, "SUSY March 2021 Summary Plot Update." ATL-PHYS-PUB-2021-007, Mar, 2021. http://cds.cern.ch/record/2758782.

[89] CMS Collaboration, "Summary plot Moriond 2017." https://twiki.cern.ch/twiki/pub/CMSPublic/SUSYSummary2017/Moriond2017_BarPlot.pdf, 2017.

[90] LEP2 SUSY WG, ALEPH, DELPHI, L3 and OPAL experiments,, "Combined LEP results." http://lepsusy.web.cern.ch/lepsusy/, 2004. Accessed: 2021-02-11.

[91] ATLAS Collaboration, "Searches for electroweak production of supersymmetric particles with compressed mass spectra in $\sqrt{s} = 13$ TeV pp collisions with the ATLAS detector," *Phys. Rev. D* **101** (2020) 052005, arXiv:1911.12606 [hep-ex].

[92] A. Buckley, "PySLHA: a Pythonic interface to SUSY Les Houches Accord data," *Eur. Phys. J. C* **75** no. 10, (2015) 467, arXiv:1305.4194 [hep-ph].

[93] CERN, *CERN Annual report 2019*. Annual Report of the European Organization for Nuclear Research. 2020. https://cds.cern.ch/record/2723123.

[94] O. S. Bruning, P. Collier, P. Lebrun, *et al.*, "LHC Design Report," *CERN Yellow Reports: Monographs* (2004) . https://cds.cern.ch/record/782076.

[95] J. P. Blewett, "200-GeV intersecting storage accelerators," in *Proceedings, 8th International Conference on High-Energy Accelerators, HEACC 1971: CERN, Geneva, Switzerland, September 20–24, 1971*. CERN, 1971. https://cds.cern.ch/record/1068131.

[96] L. Evans and P. Bryant, "LHC Machine," *JINST* **3** (2008) S08001.

[97] J. Lettry, R. Scrivens, M. Kronberger, *et al.*, "Overview of the Status and Developments on Primary Ion Sources at CERN," *Conf. Proc. C* **110904** (2011) 3474–3476.

[98] M. Vretenar, J. Vollaire, R. Scrivens, *et al.*, "Linac4 design report," *CERN Yellow Reports: Monographs* **6** (2020) . https://cds.cern.ch/record/2736208.

[99] E. Mobs, "The CERN accelerator complex - 2019. Complexe des accélérateurs du CERN - 2019,". https://cds.cern.ch/record/2684277.

[100] ATLAS Collaboration, "The ATLAS Experiment at the CERN Large Hadron Collider," *JINST* **3** (2008) S08003.

[101] CMS Collaboration, "The CMS Experiment at the CERN LHC," *JINST* **3** (2008) S08004.

[102] ALICE Collaboration, "The ALICE experiment at the CERN LHC," *JINST* **3** (2008) S08002.

[103] LHCb Collaboration, "The LHCb Detector at the LHC," *JINST* **3** (2008) S08005.

[104] TOTEM Collaboration, "The TOTEM experiment at the CERN Large Hadron Collider," *JINST* **3** (2008) S08007.

[105] LHCf Collaboration, "LHCf experiment: Technical Design Report,". https://cds.cern.ch/record/926196.

[106] MoEDAL Collaboration Collaboration, "Technical Design Report of the MoEDAL Experiment,". https://cds.cern.ch/record/1181486.

[107] ATLAS Collaboration, "ATLAS Public Results - Luminosity Public Results Run 2,". https://twiki.cern.ch/twiki/bin/view/AtlasPublic/LuminosityPublicResultsRun2. Accessed: 2021-01-17.

[108] ATLAS Collaboration, Z. Marshall, "Simulation of Pile-up in the ATLAS Experiment," *J. Phys. Conf. Ser.* **513** (2014) 022024.

[109] CERN, "First beam in the LHC - accelerating science,". https://home.cern/news/news/accelerators/record-luminosity-well-done-lhc. Accessed: 2021-01-10.

[110] ATLAS Collaboration, "Luminosity determination in pp collisions at $\sqrt{s}$ = 13 TeV using the ATLAS detector at the LHC." ATLAS-CONF-2019-021, Jun, 2019. https://cds.cern.ch/record/2677054.

[111] ATLAS Collaboration, "Luminosity determination in pp collisions at $\sqrt{s}$ = 8 TeV using the ATLAS detector at the LHC," *Eur. Phys. J. C* **76** no. 12, (2016) 653, arXiv:1608.03953 [hep-ex].

[112] G. Avoni, M. Bruschi, G. Cabras, *et al.*, "The new LUCID-2 detector for luminosity measurement and monitoring in ATLAS," *JINST* **13** no. 07, (2018) P07017.

[113] S. van der Meer, "Calibration of the effective beam height in the ISR." CERN-ISR-PO-68-31, 1968. https://cds.cern.ch/record/296752.

[114] P. Grafström and W. Kozanecki, "Luminosity determination at proton colliders," *Prog. Part. Nucl. Phys.* **81** (2015) 97–148. 52 p.

[115] M. Bajko, F. Bertinelli, N. Catalan-Lasheras, *et al.*, "Report of the Task Force on the Incident of 19th September 2008 at the LHC." CERN-LHC-PROJECT-Report-1168, Mar, 2009. https://cds.cern.ch/record/1168025.

[116] CERN, "New schedule for CERN's accelerators and experiments,". https://home.cern/news/press-release/cern/first-beam-lhc-accelerating-science. Accessed: 2021-01-10.

[117] ATLAS Collaboration, "Luminosity Determination in pp Collisions at $\sqrt{s}$ = 7 TeV Using the ATLAS Detector at the LHC," *Eur. Phys. J. C* **71** (2011) 1630, arXiv:1101.2185 [hep-ex].

[118] ATLAS Collaboration, "Improved luminosity determination in pp collisions at $\sqrt{s}$ = 7 TeV using the ATLAS detector at the LHC.," *Eur. Phys. J. C* **73** no. CERN-PH-EP-2013-026, (Feb, 2013) 2518. 27 p.

[119] CERN, "Record luminosity: well done LHC,". https://home.cern/news/news/accelerators/new-schedule-cerns-accelerators-and-experiments. Accessed: 2021-01-10.

[120] CERN, "New schedule for CERN's accelerators and experiments," November, 2020. https://home.cern/news/news/accelerators/new-schedule-cerns-accelerators-and-experiments. Accessed: 2021-03-12.

[121] G. Apollinari, I. Béjar Alonso, O. Brüning, *et al.*, eds., *High-Luminosity Large Hadron Collider (HL-LHC): Technical Design Report V. 0.1*. CERN Yellow Reports: Monographs. CERN, 2017. https://cds.cern.ch/record/2284929.

[122] J. Pequenao, "Computer generated image of the whole ATLAS detector," Mar, 2008. https://cds.cern.ch/record/1095924.

[123] ATLAS Collaboration, "ATLAS detector and physics performance: Technical Design Report, 1,". https://cds.cern.ch/record/391176.

[124] J. Pequenao, "Computer generated image of the ATLAS inner detector," Mar, 2008. https://cds.cern.ch/record/1095926.

[125] K. Potamianos, "The upgraded Pixel detector and the commissioning of the Inner Detector tracking of the ATLAS experiment for Run-2 at the Large Hadron Collider," *PoS* **EPS-HEP2015** (2015) 261, arXiv:1608.07850 [physics.ins-det].

[126] ATLAS IBL Collaboration, "Production and Integration of the ATLAS Insertable B-Layer," *JINST* **13** no. 05, (2018) T05008, arXiv:1803.00844 [physics.ins-det].

[127] ATLAS Collaboration, "ATLAS Insertable B-Layer Technical Design Report," CERN-LHCC-2010-013. http://cds.cern.ch/record/1291633.

[128] ATLAS Collaboration, "ATLAS b-jet identification performance and efficiency measurement with $t\bar{t}$ events in pp collisions at $\sqrt{s}$ = 13 TeV," *Eur. Phys. J. C* **79** no. 11, (2019) 970, arXiv:1907.05120 [hep-ex].

[129] ATLAS Collaboration, "Particle Identification Performance of the ATLAS Transition Radiation Tracker." ATLAS-CONF-2011-128, 2011. https://cds.cern.ch/record/1383793.

[130] J. Pequenao, "Computer Generated image of the ATLAS calorimeter," Mar, 2008. https://cds.cern.ch/record/1095927.

[131] J. Pequenao, "Computer generated image of the ATLAS Muons subsystem," Mar, 2008. https://cds.cern.ch/record/1095929.

[132] S. Lee, M. Livan, and R. Wigmans, "Dual-Readout Calorimetry," *Rev. Mod. Phys.* **90** no. 2, (2018) 025002, arXiv:1712.05494 [physics.ins-det].

[133] M. Leite, "Performance of the ATLAS Zero Degree Calorimeter." ATL-FWD-PROC-2013-001, Nov, 2013. https://cds.cern.ch/record/1628749.

[134] S. A. Khalek, B. Allongue, F. Anghinolfi, *et al.*, "The ALFA Roman Pot Detectors of ATLAS," *JINST* **11** no. 11, (2016) P11013, arXiv:1609.00249 [physics.ins-det].

[135] U. Amaldi, G. Cocconi, A. Diddens, *et al.*, "The Real Part of the Forward Proton Proton Scattering Amplitude Measured at the CERN Intersecting Storage Rings," *Phys. Lett. B* **66** (1977) 390–394.

[136] L. Adamczyk, E. Banaś, A. Brandt, *et al.*, "Technical Design Report for the ATLAS Forward Proton Detector." CERN-LHCC-2015-009, May, 2015. https://cds.cern.ch/record/2017378.

[137] ATLAS Collaboration, A. R. Martínez, "The Run-2 ATLAS Trigger System," *J. Phys. Conf. Ser.* **762** no. 1, (2016) 012003.

[138] ATLAS Collaboration, "ATLAS level-1 trigger: Technical Design Report." CERN-LHCC-98-014, 1998. https://cds.cern.ch/record/381429.

[139] ATLAS Collaboration, "Operation of the ATLAS trigger system in Run 2," *JINST* **15** no. 10, (2020) P10004, arXiv:2007.12539 [physics.ins-det].

[140] ATLAS Collaboration, "ATLAS high-level trigger, data-acquisition and controls: Technical Design Report,". https://cds.cern.ch/record/616089.

[141] ATLAS Collaboration, "The ATLAS Simulation Infrastructure," *Eur. Phys. J. C* **70** (2010) 823–874, arXiv:1005.4568 [physics.ins-det].

[142] T. Gleisberg, S. Hoeche, F. Krauss, *et al.*, "Event generation with SHERPA 1.1," *JHEP* **02** (2009) 007, arXiv:0811.4622 [hep-ph].

[143] A. Buckley, J. Butterworth, S. Gieseke, *et al.*, "General-purpose event generators for LHC physics," *Phys. Rept.* **504** (2011) 145–233, arXiv:1101.2599 [hep-ph].

[144] V. N. Gribov and L. N. Lipatov, "Deep inelastic e p scattering in perturbation theory," *Sov. J. Nucl. Phys.* **15** (1972) 438–450. https://cds.cern.ch/record/427157.

[145] J. Blumlein, T. Doyle, F. Hautmann, *et al.*, "Structure functions in deep inelastic scattering at HERA," in *Workshop on Future Physics at HERA*. 9, 1996. arXiv:hep-ph/9609425.

[146] A. Buckley, J. Ferrando, S. Lloyd, *et al.*, "LHAPDF6: parton density access in the LHC precision era," *Eur. Phys. J. C* **75** (2015) 132, arXiv:1412.7420 [hep-ph].

[147] M. Bengtsson and T. Sjostrand, "Coherent Parton Showers Versus Matrix Elements: Implications of PETRA - PEP Data," *Phys. Lett. B* **185** (1987) 435.

[148] S. Catani, F. Krauss, R. Kuhn, and B. R. Webber, "QCD matrix elements + parton showers," *JHEP* **11** (2001) 063, arXiv:hep-ph/0109231.

[149] L. Lonnblad, "Correcting the color dipole cascade model with fixed order matrix elements," *JHEP* **05** (2002) 046, arXiv:hep-ph/0112284.

[150] B. Andersson, G. Gustafson, G. Ingelman, and T. Sjostrand, "Parton Fragmentation and String Dynamics," *Phys. Rept.* **97** (1983) 31–145.

[151] B. Andersson, *The Lund Model*. Cambridge Monographs on Particle Physics, Nuclear Physics and Cosmology. Cambridge University Press, 1998.

[152] D. Amati and G. Veneziano, "Preconfinement as a Property of Perturbative QCD," *Phys. Lett. B* **83** (1979) 87–92.

[153] D. Yennie, S. Frautschi, and H. Suura, "The infrared divergence phenomena and high-energy processes," *Annals Phys.* **13** no. 3, (1961) 379–452.

[154] M. Dobbs and J. B. Hansen, "The HepMC C++ Monte Carlo event record for High Energy Physics," *Comput. Phys. Commun.* **134** (2001) 41–46.

[155] GEANT4 Collaboration, "GEANT4: A Simulation toolkit," *Nucl. Instrum. Meth.* **A506** (2003) 250–303.

[156] ATLAS Collaboration, "The new Fast Calorimeter Simulation in ATLAS." ATL-SOFT-PUB-2018-002, Jul, 2018. https://cds.cern.ch/record/2630434.

[157] K. Cranmer, "Practical Statistics for the LHC," in *2011 European School of High-Energy Physics*, pp. 267–308. 2014. arXiv:1503.07622 [physics.data-an].

[158] G. Cowan, K. Cranmer, E. Gross, and O. Vitells, "Asymptotic formulae for likelihood-based tests of new physics," *Eur. Phys. J.* **C71** (2011) 1554, arXiv:1007.1727 [physics.data-an]. [Erratum: Eur. Phys. J. C 73, 2501 (2013)].

[159] ATLAS Collaboration, "Reproducing searches for new physics with the ATLAS experiment through publication of full statistical likelihoods." ATL-PHYS-PUB-2019-029, 2019. https://cds.cern.ch/record/2684863.

[160] ROOT Collaboration, K. Cranmer, G. Lewis, L. Moneta, *et al.*, "HistFactory: A tool for creating statistical models for use with RooFit and RooStats,". https://cds.cern.ch/record/1456844.

[161] W. Verkerke and D. P. Kirkby, "The RooFit toolkit for data modeling," *eConf* **C0303241** (2003) MOLT007, arXiv:physics/0306116.

[162] F. James and M. Roos, "Minuit: A System for Function Minimization and Analysis of the Parameter Errors and Correlations," *Comput. Phys. Commun.* **10** (1975) 343–367. https://cds.cern.ch/record/310399.

[163] L. Moneta, K. Belasco, K. S. Cranmer, *et al.*, "The RooStats Project," *PoS* **ACAT2010** (2010) 057, arXiv:1009.1003 [physics.data-an].

[164] R. Brun and F. Rademakers, "ROOT: An object oriented data analysis framework," *Nucl. Instrum. Meth.* **A389** (1997) 81–86.

[165] I. Antcheva *et al.*, "ROOT — A C++ framework for petabyte data storage, statistical analysis and visualization," *Computer Physics Communications* **182** no. 6, (2011) 1384 – 1385.

[166] M. Baak, G. J. Besjes, D. Côte, A. Koutsman, J. Lorenz, D. Short, "HistFitter software framework for statistical data analysis," *Eur. Phys. J.* **C75** (2015) 153, arXiv:1410.1280 [hep-ex].

[167] L. Heinrich, M. Feickert, G. Stark, and K. Cranmer, "pyhf: pure-Python implementation of HistFactory statistical models," *Journal of Open Source Software* **6** no. 58, (2021) 2823.

[168] L. Heinrich, M. Feickert, and G. Stark, "pyhf: v0.6.0," Version 0.6.0. https://github.com/scikit-hep/pyhf.

[169] C. R. Harris, K. J. Millman, S. J. van der Walt, *et al.*, "Array programming with NumPy," *Nature* **585** no. 7825, (Sept., 2020) 357–362.

[170] A. Paszke, S. Gross, F. Massa, *et al.*, "Pytorch: An imperative style, high-performance deep learning library," *Adv. Neural Inf. Process. Syst.* **32** (2019) 8024–8035, arXiv:1912.01703 [cs.LG].

[171] M. Abadi, A. Agarwal, P. Barham, *et al.*, "TensorFlow: Large-scale machine learning on heterogeneous systems," 2015. https://www.tensorflow.org/. Software available from tensorflow.org.

[172] J. Bradbury, R. Frostig, P. Hawkins, *et al.*, "JAX: composable transformations of Python+NumPy programs," Version 0.1.46, 2018. http://github.com/google/jax.

[173] S. S. Wilks, "The large-sample distribution of the likelihood ratio for testing composite hypotheses," *Ann. Math. Statist.* **9** no. 1, (03, 1938) 60–62.

[174] A. Wald, "Tests of statistical hypotheses concerning several parameters when the number of observations is large," *Trans. Am. Math. Soc.* **54** no. 3, (1943) 426–482.

[175] G. Cowan, "Statistics for Searches at the LHC," in *69th Scottish Universities Summer School in Physics: LHC Physics*, pp. 321–355. 7, 2013. arXiv:1307.2487 [hep-ex].

[176] A. L. Read, "Presentation of search results: the CL_S technique," *J. Phys. G* **28** (2002) 2693.

[177] R. D. Cousins, J. T. Linnemann, and J. Tucker, "Evaluation of three methods for calculating statistical significance when incorporating a systematic uncertainty into a test of the background-only hypothesis for a Poisson process," *Nucl. Instrum. Meth. A* **595** no. 2, (2008) 480, arXiv:physics/0702156 [physics.data-an].

[178] K. Cranmer, "Statistical challenges for searches for new physics at the LHC," in *Statistical Problems in Particle Physics, Astrophysics and Cosmology*. 9, 2005. arXiv:physics/0511028.

[179] ATLAS Collaboration, "Search for direct pair production of a chargino and a neutralino decaying to the 125 GeV Higgs boson in $\sqrt{s} = 8$ TeV pp collisions with the ATLAS detector," *Eur. Phys. J. C* **75** (2015) 208, arXiv:1501.07110 [hep-ex].

[180] ATLAS Collaboration, "Search for chargino and neutralino production in final states with a Higgs boson and missing transverse momentum at $\sqrt{s} = 13$ TeV with the ATLAS detector," *Phys. Rev. D* **100** (2019) 012006, arXiv:1812.09432 [hep-ex].

[181] CMS Collaboration, "Search for electroweak production of charginos and neutralinos in WH events in proton–proton collisions at $\sqrt{s} = 13$ TeV," *JHEP* **11** (2017) 029, arXiv:1706.09933 [hep-ex].

[182] ATLAS Collaboration, "Search for direct production of electroweakinos in final states with one lepton, missing transverse momentum and a Higgs boson decaying into two b-jets in pp collisions at $\sqrt{s} = 13$ TeV with the ATLAS detector," *Eur. Phys. J. C* **80** (2020) 691, arXiv:1909.09226 [hep-ex].

[183] ATLAS Collaboration, "Improvements in $t\bar{t}$ modelling using NLO+PS Monte Carlo generators for Run 2." ATL-PHYS-PUB-2018-009, 2018. https://cds.cern.ch/record/2630327.

[184] ATLAS Collaboration, "Modelling of the $t\bar{t}H$ and $t\bar{t}V(V = W, Z)$ processes for $\sqrt{s} = 13$ TeV ATLAS analyses." ATL-PHYS-PUB-2016-005, 2016. https://cds.cern.ch/record/2120826.

[185] ATLAS Collaboration, "ATLAS simulation of boson plus jets processes in Run 2." ATL-PHYS-PUB-2017-006, 2017. https://cds.cern.ch/record/2261937.

[186] ATLAS Collaboration, "Multi-Boson Simulation for 13 TeV ATLAS Analyses." ATL-PHYS-PUB-2017-005, 2017. https://cds.cern.ch/record/2261933.

[187] J. Alwall, R. Frederix, S. Frixione, *et al.*, "The automated computation of tree-level and next-to-leading order differential cross sections, and their matching to parton shower simulations," *JHEP* **07** (2014) 079, arXiv:1405.0301 [hep-ph].

[188] R. Frederix and S. Frixione, "Merging meets matching in MC@NLO," *JHEP* **12** (2012) 061, arXiv:1209.6215 [hep-ph].

[189] NNPDF Collaboration, "Parton distributions with LHC data," *Nucl. Phys. B* **867** (2013) 244, arXiv:1207.1303 [hep-ph].

[190] T. Sjöstrand, S. Ask, J. R. Christiansen, *et al.*, "An Introduction to PYTHIA 8.2," *Comput. Phys. Commun.* **191** (2015) 159–177, arXiv:1410.3012 [hep-ph].

[191] ATLAS Collaboration, "ATLAS Pythia 8 tunes to 7 TeV data." ATL-PHYS-PUB-2014-021, 2014. https://cds.cern.ch/record/1966419.

[192] L. Lönnblad and S. Prestel, "Matching tree-level matrix elements with interleaved showers," *JHEP* **03** (2012) 019, arXiv:1109.4829 [hep-ph].

[193] D. J. Lange, "The EvtGen particle decay simulation package," *Nucl. Instrum. Meth. A* **462** (2001) 152.

[194] ATLAS Collaboration, "The Pythia 8 A3 tune description of ATLAS minimum bias and inelastic measurements incorporating the Donnachie–Landshoff diffractive model." ATL-PHYS-PUB-2016-017, 2016. https://cds.cern.ch/record/2206965.

[195] B. Fuks, M. Klasen, D. R. Lamprea, and M. Rothering, "Precision predictions for electroweak superpartner production at hadron colliders with RESUMMINO," *Eur. Phys. J. C* **73** (2013) 2480, arXiv:1304.0790 [hep-ph].

[196] S. Alioli, P. Nason, C. Oleari, and E. Re, "A general framework for implementing NLO calculations in shower Monte Carlo programs: the POWHEG BOX," *JHEP* **06** (2010) 043, arXiv:1002.2581 [hep-ph].

[197] S. Frixione, P. Nason, and G. Ridolfi, "A Positive-weight next-to-leading-order Monte Carlo for heavy flavour hadroproduction," *JHEP* **09** (2007) 126, arXiv:0707.3088 [hep-ph].

[198] P. Nason, "A New method for combining NLO QCD with shower Monte Carlo algorithms," *JHEP* **11** (2004) 040, arXiv:hep-ph/0409146.

[199] E. Bothmann *et al.*, "Event generation with Sherpa 2.2," *SciPost Phys.* **7** no. 3, (2019) 034, arXiv:1905.09127 [hep-ph].

[200] NNPDF Collaboration, "Parton distributions for the LHC run II," *JHEP* **04** (2015) 040, arXiv:1410.8849 [hep-ph].

[201] M. Czakon and A. Mitov, "Top++: A program for the calculation of the top-pair cross-section at hadron colliders," *Comput. Phys. Commun.* **185** (2014) 2930, arXiv:1112.5675 [hep-ph].

[202] M. Cacciari, M. Czakon, M. Mangano, *et al.*, "Top-pair production at hadron colliders with next-to-next-to-leading logarithmic soft-gluon resummation," *Phys. Lett. B* **710** (2012) 612–622, arXiv:1111.5869 [hep-ph].

[203] P. Kant, O. M. Kind, T. Kintscher, *et al.*, "HatHor for single top-quark production: Updated predictions and uncertainty estimates for single top-quark production in hadronic collisions," *Comput. Phys. Commun.* **191** (2015) 74–89, arXiv:1406.4403 [hep-ph].

[204] N. Kidonakis, "Two-loop soft anomalous dimensions for single top quark associated production with a W^- or H^-," *Phys. Rev. D* **82** (2010) 054018, arXiv:1005.4451 [hep-ph].

[205] J. M. Campbell and R. K. Ellis, "$t\bar{t}W^{+-}$ production and decay at NLO," *JHEP* **07** (2012) 052, arXiv:1204.5678 [hep-ph].

[206] A. Lazopoulos, T. McElmurry, K. Melnikov, and F. Petriello, "Next-to-leading order QCD corrections to $t\bar{t}Z$ production at the LHC," *Phys. Lett. B* **666** (2008) 62–65, arXiv:0804.2220 [hep-ph].

[207] R. Gavin, Y. Li, F. Petriello, and S. Quackenbush, "FEWZ 2.0: A code for hadronic Z production at next-to-next-to-leading order," arXiv:1011.3540 [hep-ph].

[208] LHC Higgs Cross Section Working Group Collaboration, "Handbook of LHC Higgs Cross Sections: 4. Deciphering the Nature of the Higgs Sector," arXiv:1610.07922 [hep-ph].

[209] ATLAS Collaboration, "Example ATLAS tunes of Pythia8, Pythia6 and Powheg to an observable sensitive to Z boson transverse momentum." ATL-PHYS-PUB-2013-017, 2013. https://cds.cern.ch/record/1629317.

[210] ATLAS Collaboration, "Performance of the ATLAS track reconstruction algorithms in dense environments in LHC Run 2," *Eur. Phys. J. C* **77** (2017) 673, arXiv:1704.07983 [hep-ex].

[211] R. Frühwirth, "Application of Kalman filtering to track and vertex fitting," *Nucl. Instrum. Meth. A* **262** (1987) 444–450.

[212] T. Cornelissen, M. Elsing, I. Gavrilenko, *et al.*, "The new ATLAS track reconstruction (NEWT)," *J. Phys.: Conf. Ser.* **119** (2008) 032014.

[213] ATLAS Collaboration, "Vertex Reconstruction Performance of the ATLAS Detector at $\sqrt{s}$ = 13 TeV." ATL-PHYS-PUB-2015-026, 2015. https://cds.cern.ch/record/2037717.

[214] ATLAS Collaboration, "Reconstruction of primary vertices at the ATLAS experiment in Run 1 proton–proton collisions at the LHC," *Eur. Phys. J. C* **77** (2017) 332, arXiv:1611.10235 [hep-ex].

[215] ATLAS Collaboration, "Topological cell clustering in the ATLAS calorimeters and its performance in LHC Run 1," *Eur. Phys. J. C* **77** (2017) 490, arXiv:1603.02934 [hep-ex].

[216] ATLAS Collaboration, "Electron and photon performance measurements with the ATLAS detector using the 2015–2017 LHC proton–proton collision data," *JINST* **14** (2019) P12006, arXiv:1908.00005 [hep-ex].

[217] ATLAS Collaboration, "Measurement of the photon identification efficiencies with the ATLAS detector using LHC Run 2 data collected in 2015 and 2016," *Eur. Phys. J. C* **79** (2019) 205, arXiv:1810.05087 [hep-ex].

[218] ATLAS Collaboration, "Electron reconstruction and identification in the ATLAS experiment using the 2015 and 2016 LHC proton–proton collision data at $\sqrt{s}$ = 13 TeV," *Eur. Phys. J. C* **79** (2019) 639, arXiv:1902.04655 [hep-ex].

[219] ATLAS Collaboration, "Muon reconstruction performance of the ATLAS detector in proton–proton collision data at $\sqrt{s}$ = 13 TeV," *Eur. Phys. J. C* **76** (2016) 292, arXiv:1603.05598 [hep-ex].

[220] ATLAS Collaboration, "Muon reconstruction and identification efficiency in ATLAS using the full Run 2 pp collision data set at $\sqrt{s}$ = 13 TeV," arXiv:2012.00578 [hep-ex].

[221] M. Cacciari, G. P. Salam, and G. Soyez, "The anti-k_t jet clustering algorithm," *JHEP* **04** (2008) 063, arXiv:0802.1189 [hep-ph].

[222] M. Cacciari, G. P. Salam, and G. Soyez, "FastJet user manual," *Eur. Phys. J. C* **72** (2012) 1896, arXiv:1111.6097 [hep-ph].

[223] M. Cacciari, "FastJet: A Code for fast k_t clustering, and more," in *41st Rencontres de Moriond: QCD and Hadronic Interactions*, pp. 487–490. 7, 2006. arXiv:hep-ph/0607071.

[224] ATLAS Collaboration, "Jet energy scale and resolution measured in proton-proton collisions at $\sqrt{s}$ = 13 TeV with the ATLAS detector." CERN-EP-2020-083, 7, 2020. arXiv:2007.02645 [hep-ex].

[225] M. Cacciari and G. P. Salam, "Pileup subtraction using jet areas," *Phys. Lett. B* **659** (2008) 119–126, arXiv:0707.1378 [hep-ph].

[226] ATLAS Collaboration, "Jet energy measurement with the ATLAS detector in proton–proton collisions at $\sqrt{s}$ = 7 TeV," *Eur. Phys. J. C* **73** (2013) 2304, arXiv:1112.6426 [hep-ex].

[227] ATLAS Collaboration, "Determination of jet calibration and energy resolution in proton-proton collisions at $\sqrt{s}$ = 8 TeV using the ATLAS detector," *Eur. Phys. J. C* **80** no. 12, (2020) 1104, arXiv:1910.04482 [hep-ex].

[228] ATLAS Collaboration, "Performance of pile-up mitigation techniques for jets in pp collisions at $\sqrt{s}$ = 8 TeV using the ATLAS detector," *Eur. Phys. J. C* **76** (2016) 581, arXiv:1510.03823 [hep-ex].

[229] ATLAS Collaboration, "Optimisation and performance studies of the ATLAS b-tagging algorithms for the 2017-18 LHC run." ATL-PHYS-PUB-2017-013, 2017. https://cds.cern.ch/record/2273281.

[230] ATLAS Collaboration, "ATLAS b-jet identification performance and efficiency measurement with $t\bar{t}$ events in pp collisions at $\sqrt{s}$ = 13 TeV," *Eur. Phys. J. C* **79** (2019) 970, arXiv:1907.05120 [hep-ex].

[231] ATLAS Collaboration, "Measurements of b-jet tagging efficiency with the ATLAS detector using $t\bar{t}$ events at $\sqrt{s}$ = 13 TeV," *JHEP* **08** (2018) 089, arXiv:1805.01845 [hep-ex].

[232] ATLAS Collaboration, "Performance of missing transverse momentum reconstruction with the ATLAS detector using proton–proton collisions at $\sqrt{s}$ = 13 TeV," *Eur. Phys. J. C* **78** (2018) 903, arXiv:1802.08168 [hep-ex].

[233] ATLAS Collaboration, "$E_{\mathrm{T}}^{\mathrm{miss}}$ performance in the ATLAS detector using 2015–2016 LHC pp collisions." ATLAS-CONF-2018-023, 2018. https://cds.cern.ch/record/2625233.

[234] D. Adams *et al.*, "Recommendations of the Physics Objects and Analysis Harmonisation Study Groups 2014." ATL-PHYS-INT-2014-018, Jul, 2014. https://cds.cern.ch/record/1743654.

[235] M. Cacciari, G. P. Salam, and G. Soyez, "The Catchment Area of Jets," *JHEP* **04** (2008) 005, arXiv:0802.1188 [hep-ph].

[236] UA1 Collaboration, "Experimental Observation of Isolated Large Transverse Energy Electrons with Associated Missing Energy at $\sqrt{s}$ = 540 GeV," *Phys. Lett. B* **122** (1983) 103–116.

[237] UA1 Collaboration, G. Arnison *et al.*, "Further Evidence for Charged Intermediate Vector Bosons at the SPS Collider," *Phys. Lett. B* **129** (1983) 273–282.

[238] U. Baur, "Measuring the W boson mass at hadron colliders," in *Mini-Workshop on Electroweak Precision Data and the Higgs Mass*. 4, 2003. arXiv:hep-ph/0304266.

[239] J. Smith, W. L. van Neerven, and J. A. M. Vermaseren, "The Transverse Mass and Width of the W Boson," *Phys. Rev. Lett.* **50** (1983) 1738.

[240] D. R. Tovey, "On measuring the masses of pair-produced semi-invisibly decaying particles at hadron colliders," *JHEP* **04** (2008) 034, arXiv:0802.2879 [hep-ph].

[241] G. Polesello and D. R. Tovey, "Supersymmetric particle mass measurement with the boost-corrected contransverse mass," *JHEP* **03** (2010) 030, arXiv:0910.0174 [hep-ph].

[242] ATLAS Collaboration, "Performance of the missing transverse momentum triggers for the ATLAS detector during Run-2 data taking," *JHEP* **08** (2020) 080, arXiv:2005.09554 [hep-ex].

[243] ATLAS Collaboration, "Performance of algorithms that reconstruct missing transverse momentum in $\sqrt{s}$ = 8 TeV proton-proton collisions in the ATLAS detector," *Eur. Phys. J. C* **77** no. 4, (2017) 241, arXiv:1609.09324 [hep-ex].

[244] ATLAS Collaboration, "ATLAS data quality operations and performance for 2015–2018 data-taking," *JINST* **15** (2020) P04003, arXiv:1911.04632 [physics.ins-det].

[245] ATLAS Collaboration, "Selection of jets produced in 13 TeV proton–proton collisions with the ATLAS detector." ATLAS-CONF-2015-029, 2015. https://cds.cern.ch/record/2037702.

[246] N. Hartmann, "ahoi: a horrible optimisation instrument." https://gitlab.com/nikoladze/ahoi, 2018.

[247] ATLAS Collaboration, "Object-based missing transverse momentum significance in the ATLAS detector,". https://cds.cern.ch/record/2630948.

[248] A. Roodman, "Blind analysis in particle physics," *eConf* **C030908** (2003) TUIT001, arXiv:physics/0312102.

[249] W. Buttinger, "Using Event Weights to account for differences in Instantaneous Luminosity and Trigger Prescale in Monte Carlo and Data." ATL-COM-SOFT-2015-119, May, 2015. https://cds.cern.ch/record/2014726.

[250] ATLAS Collaboration, "Measurement of the Inelastic Proton–Proton Cross Section at $\sqrt{s} = 13$ TeV with the ATLAS Detector at the LHC," *Phys. Rev. Lett.* **117** (2016) 182002, arXiv:1606.02625 [hep-ex].

[251] ATLAS Collaboration, "A method for the construction of strongly reduced representations of ATLAS experimental uncertainties and the application thereof to the jet energy scale." ATL-PHYS-PUB-2015-014, 2015. https://cds.cern.ch/record/2037436.

[252] J. Bellm *et al.*, "Herwig 7.0/Herwig++ 3.0 release note," *Eur. Phys. J.* **C76** no. 4, (2016) 196, arXiv:1512.01178 [hep-ph].

[253] ATLAS Collaboration, "Simulation of top-quark production for the ATLAS experiment at $\sqrt{s} = 13$ TeV." ATL-PHYS-PUB-2016-004, 2016. https://cds.cern.ch/record/2120417.

[254] S. Frixione, E. Laenen, P. Motylinski, *et al.*, "Single-top hadroproduction in association with a W boson," *JHEP* **07** (2008) 029, arXiv:0805.3067 [hep-ph].

[255] CMS Collaboration, "Search for chargino-neutralino production in final states with a Higgs boson and a W boson." CMS-PAS-SUS-20-003, 2021. https://cds.cern.ch/record/2758360.

[256] ATLAS Collaboration, "Search for electroweak production of charginos and sleptons decaying into final states with two leptons and missing transverse momentum in $\sqrt{s} = 13$ TeV pp collisions using the ATLAS detector," *Eur. Phys. J. C* **80** (2020) 123, arXiv:1908.08215 [hep-ex].

[257] X. Chen, S. Dallmeier-Tiessen, R. Dasler, *et al.*, "Open is not enough," *Nature Physics* **15** no. 2, (Feb, 2019) 113–119.

[258] LHC Reinterpretation Forum Collaboration, "Reinterpretation of LHC Results for New Physics: Status and Recommendations after Run 2," *SciPost Phys.* **9** no. 2, (2020) 022, arXiv:2003.07868 [hep-ph].

[259] ATLAS Collaboration, "RECAST framework reinterpretation of an ATLAS Dark Matter Search constraining a model of a dark Higgs boson decaying to two b-quarks." ATL-PHYS-PUB-2019-032, 2019. https://cds.cern.ch/record/2686290.

[260] K. Cranmer and I. Yavin, "RECAST: Extending the Impact of Existing Analyses," *JHEP* **04** (2011) 038, arXiv:1010.2506 [hep-ex].

[261] D. Dercks, N. Desai, J. S. Kim, *et al.*, "CheckMATE 2: From the model to the limit," *Comput. Phys. Commun.* **221** (2017) 383–418, arXiv:1611.09856 [hep-ph].

[262] M. Drees, H. Dreiner, D. Schmeier, *et al.*, "CheckMATE: Confronting your Favourite New Physics Model with LHC Data," *Comput. Phys. Commun.* **187** (2015) 227–265, arXiv:1312.2591 [hep-ph].

[263] E. Conte, B. Fuks, and G. Serret, "MadAnalysis 5, A User-Friendly Framework for Collider Phenomenology," *Comput. Phys. Commun.* **184** (2013) 222–256, arXiv:1206.1599 [hep-ph].

[264] E. Maguire, L. Heinrich, and G. Watt, "HEPData: a repository for high energy physics data," *J. Phys. Conf. Ser.* **898** no. 10, (2017) 102006, arXiv:1704.05473 [hep-ex].

[265] ATLAS Collaboration, "SimpleAnalysis: Simplified ATLAS SUSY analysis framework." https://gitlab.cern.ch/atlas-sa/simple-analysis, 2021.

[266] S. Ovyn, X. Rouby, and V. Lemaitre, "DELPHES, a framework for fast simulation of a generic collider experiment," arXiv:0903.2225 [hep-ph].

[267] A. Buckley, J. Butterworth, D. Grellscheid, *et al.*, "Rivet user manual," *Comput. Phys. Commun.* **184** (2013) 2803–2819, arXiv:1003.0694 [hep-ph].

[268] A. Buckley, D. Kar, and K. Nordström, "Fast simulation of detector effects in Rivet," *SciPost Phys.* **8** (2020) 025, arXiv:1910.01637 [hep-ph].

[269] S. Kraml, S. Kulkarni, U. Laa, *et al.*, "SModelS: a tool for interpreting simplified-model results from the LHC and its application to supersymmetry," *Eur. Phys. J. C* **74** (2014) 2868, arXiv:1312.4175 [hep-ph].

[270] F. Ambrogi, S. Kraml, S. Kulkarni, *et al.*, "SModelS v1.1 user manual: Improving simplified model constraints with efficiency maps," *Comput. Phys. Commun.* **227** (2018) 72–98, arXiv:1701.06586 [hep-ph].

[271] ATLAS Collaboration, "HEPData record for SUSY-2019-08 analysis data,". https://www.hepdata.net/record/ins1755298?version=4.

[272] ATLAS Collaboration, "Full likelihood of susy-2019-08: 1lbb-likelihoods-hepdata.tar.gz," 2020. https://www.hepdata.net/record/resource/1408476?view=true.

[273] G. Alguero, S. Kraml, and W. Waltenberger, "A SModelS interface for pyhf likelihoods," arXiv:2009.01809 [hep-ph].

[274] M. D. Goodsell, "Implementation of the ATLAS-SUSY-2019-08 analysis in the MadAnalysis 5 framework (electroweakinos with a Higgs decay into a $b\bar{b}$ pair, one lepton and missing transverse energy; 139 fb^{-1})," *Mod. Phys. Lett. A* **36** no. 01, (2021) 2141006.

[275] J. Y. Araz *et al.*, "Proceedings of the second MadAnalysis 5 workshop on LHC recasting in Korea," *Mod. Phys. Lett. A* **36** no. 01, (2021) 2102001, arXiv:2101.02245 [hep-ph].

[276] M. Feickert, L. Heinrich, G. Stark, and B. Galewsky, "Distributed statistical inference with pyhf enabled through funcX," in *25th International Conference on Computing in High-Energy and Nuclear Physics*. 3, 2021. arXiv:2103.02182 [cs.DC].

[277] R. Chard, Y. Babuji, Z. Li, *et al.*, "funcx: A federated function serving fabric for science," in *Proceedings of the 29th International Symposium on High-Performance Parallel and Distributed Computing*. ACM, Jun, 2020. arXiv:2005.04215 [cs.DC].

[278] D. Merkel, "Docker: Lightweight linux containers for consistent development and deployment," *Linux J.* **2014** no. 239, (Mar., 2014) .

[279] S. Binet and B. Couturier, "Docker & HEP: Containerization of applications for development, distribution and preservation," *J. Phys.: Conf. Ser.* **664** no. 2, (2015) 022007. 8 p.

[280] E. R. Gansner and S. C. North, "An open graph visualization system and its applications to software engineering," *Softw. Pract. Exper.* **30** no. 11, (Sept., 2000) 1203–1233.

[281] E. R. Gansner, Y. Koren, and S. North, "Graph drawing by stress majorization," in *Graph Drawing*, J. Pach, ed., pp. 239–250. Springer, Berlin, 2005.

[282] K. Cranmer and L. Heinrich, "Yadage and Packtivity - analysis preservation using parametrized workflows," *J. Phys. Conf. Ser.* **898** no. 10, (2017) 102019, arXiv:1706.01878 [physics.data-an].

[283] ATLAS Collaboration, "Electron and photon energy calibration with the ATLAS detector using 2015–2016 LHC proton–proton collision data," *JINST* **14** (2019) P03017, arXiv:1812.03848 [hep-ex].

[284] E. Schanet, J. M. Lorenz, G. H. Stark, and L. A. Heinrich, "Simplified likelihoods for searches for supersymmetry." ATL-COM-PHYS-2021-124, Mar, 2021. https://cds.cern.ch/record/2758958.

[285] E. Schanet, "Simplify: Create and validate simplified likelihoods," Version 0.1.5. https://github.com/eschanet/simplify.

[286] E. Schanet, "Simplified likelihood for SUSY-2019-08," Version 0.0.1. https://github.com/eschanet/simplify/blob/6ba1586ae009faab5e5da4f7ac29c4385a6f751f/examples/ANA-SUSY-2019-08/simplify_BkgOnly.json.

[287] P. C. Bryan and M. Nottingham, "Javascript object notation (json) patch," Version RFC 6902, Apr, 2013. https://www.rfc-editor.org/rfc/rfc6902.txt.

[288] ATLAS Collaboration, "Search for direct stau production in events with two hadronic τ-leptons in $\sqrt{s} = 13$ TeV pp collisions with the ATLAS detector," *Phys. Rev. D* **101** (2020) 032009, arXiv:1911.06660 [hep-ex].

[289] ATLAS Collaboration, "Search for bottom-squark pair production with the ATLAS detector in final states containing Higgs bosons, b-jets and missing transverse momentum," *JHEP* **12** (2019) 060, arXiv:1908.03122 [hep-ex].

[290] W. Porod, "SPheno, a program for calculating supersymmetric spectra, SUSY particle decays and SUSY particle production at e+ e- colliders," *Comput. Phys. Commun.* **153** (2003) 275–315, arXiv:hep-ph/0301101.

[291] W. Porod and F. Staub, "SPheno 3.1: Extensions including flavour, CP-phases and models beyond the MSSM," *Comput. Phys. Commun.* **183** (2012) 2458–2469, arXiv:1104.1573 [hep-ph].

[292] S. Heinemeyer, W. Hollik, and G. Weiglein, "FeynHiggs: A Program for the calculation of the masses of the neutral CP even Higgs bosons in the MSSM," *Comput. Phys. Commun.* **124** (2000) 76–89, arXiv:hep-ph/9812320.

[293] H. Bahl, T. Hahn, S. Heinemeyer, *et al.*, "Precision calculations in the MSSM Higgs-boson sector with FeynHiggs 2.14," *Comput. Phys. Commun.* **249** (2020) 107099, arXiv:1811.09073 [hep-ph].

[294] T. Hahn, S. Heinemeyer, W. Hollik, *et al.*, "High-Precision Predictions for the Light CP -Even Higgs Boson Mass of the Minimal Supersymmetric Standard Model," *Phys. Rev. Lett.* **112** no. 14, (2014) 141801, arXiv:1312.4937 [hep-ph].

[295] B. C. Allanach, "SOFTSUSY: a program for calculating supersymmetric spectra," *Comput. Phys. Commun.* **143** (2002) 305–331, arXiv:hep-ph/0104145 [hep-ph].

[296] G. Belanger, F. Boudjema, A. Pukhov, and A. Semenov, "MicrOMEGAs 2.0: A Program to calculate the relic density of dark matter in a generic model," *Comput. Phys. Commun.* **176** (2007) 367–382, arXiv:hep-ph/0607059.

[297] G. Belanger, F. Boudjema, A. Pukhov, and A. Semenov, "micrOMEGAs: A Tool for dark matter studies," *Nuovo Cim. C* **033N2** (2010) 111–116, arXiv:1005.4133 [hep-ph].

[298] W. Beenakker, R. Hopker, and M. Spira, "PROSPINO: A Program for the Production of Supersymmetric Particles in Next-to-leading Order QCD," arXiv:hep-ph/9611232 [hep-ph]. https://cds.cern.ch/record/314229.

[299] W. Beenakker, M. Klasen, M. Kramer, *et al.*, "The Production of charginos / neutralinos and sleptons at hadron colliders," *Phys. Rev. Lett.* **83** (1999) 3780–3783, arXiv:hep-ph/9906298. [Erratum: Phys. Rev. Lett. 100, 029901 (2008)].

[300] ATLAS Collaboration, "Search for long-lived charginos based on a disappearing-track signature using 136 fb^{-1} of pp collisions at $\sqrt{s}$ = 13 TeV with the ATLAS detector." ATLAS-CONF-2021-015, Mar, 2021. https://cds.cern.ch/record/2759676.

[301] A. Arbey, M. Battaglia, and F. Mahmoudi, "Higgs Production in Neutralino Decays in the MSSM - The LHC and a Future e^+e^- Collider," *Eur. Phys. J. C* **75** no. 3, (2015) 108, arXiv:1212.6865 [hep-ph].

[302] M. E. Cabrera, J. A. Casas, A. Delgado, *et al.*, "Naturalness of MSSM dark matter," *JHEP* **08** (2016) 058, arXiv:1604.02102 [hep-ph].

[303] N. Arkani-Hamed, G. L. Kane, J. Thaler, and L.-T. Wang, "Supersymmetry and the LHC inverse problem," *JHEP* **08** (2006) 070, arXiv:hep-ph/0512190.

[304] S. Amari, *Differential-Geometrical Methods in Statistics*. Springer New York, New York, NY, 1985.

[305] J. Brehmer, K. Cranmer, F. Kling, and T. Plehn, "Better Higgs boson measurements through information geometry," *Phys. Rev. D* **95** no. 7, (2017) 073002, arXiv:1612.05261 [hep-ph].

[306] ATLAS Collaboration, "Summary of the searches for squarks and gluinos using $\sqrt{s}$ = 8 TeV pp collisions with the ATLAS experiment at the LHC," *JHEP* **10** (2015) 054, arXiv:1507.05525 [hep-ex].

[307] ATLAS Collaboration, "Search for the electroweak production of supersymmetric particles in $\sqrt{s}$ = 8 TeV pp collisions with the ATLAS detector," *Phys. Rev. D* **93** (2016) 052002, arXiv:1509.07152 [hep-ex].